Treball de Fi de Màster

Master's Degree in Automatic Control and Robotics (MUAR)

Coordination of Autonomous Vehicles Considering Safety Mechanisms

Autor: Álvaro Carrizosa Rendón

Director: Dr. Vicenç Puig Cayuela

Convocatòria: September 2022

Escola Tècnica Superior
d'Enginyeria Industrial de Barcelona

Contents

ETSEIB

Acknowledgements

Completing this work means the end of a stage in my life and I would like to thank all those people who have allowed it for their support.
Firstly, to the staff of the ETSEIB, because without them, it would be impossible the day-to-day at the university. I am also infinitely grateful to all the professors for teaching me the relevance of engineering and its power to change the world. But above all, to Professor Vicenç Puig, for having trusted me to carry out research support tasks with an INIREC grant during the first year and subsequently allowing me to do the TFM with him. For his availability and dedication both in class and in the office, and for transmitting my colleagues and me his passion for automatic control and research.
Secondly, I also want to thank my classmates, my flatmates and friends. They are the ones who have supported me both academically and personally and have shown me along these years that they will continue to be by my side in future stages.
Finally, I want to thank my family, which has always played an important role. To my father, for having been able to transmit to me the beauty of research and science since I was little, having supported me in every step I have taken in this direction. To my mother and my sister, who are my references for both effort and perseverance, being my main support in the best and worst moments of my entire university stage. To my grandmother from Cádiz, for being always so proud of my progress. To my grandparents from Sevilla, because they taught me that age is not a problem for using technology, and the importance of making an effort in studies. And specially because I know that no one would have been so happy and proud of me if they had had the opportunity to see me finishing my studies.

Thank you,
Barcelona, September 2022.
Álvaro Carrizosa Rendón.

List of Figures

Index of Notation

Acronym

ESAII Enginyeria de Sistemes Automàtica i Informàtica Industrial

LPV Linear Parameter Varying

MP Motion Planner

MPC Model Predictive Controller

NL Non Linear

ODE Ordinary differential equations system

ROS Robotic Operating System (set of libraries)

TFM Treball de Fi de Màster

V2I Vehicle to infrastructure communication

V2V Vehicle to vehicle communication

V2X Vehicle to everything communication

Optimization Problem Notation

$\Delta u_{min}, \Delta u_{max}$ Lower and upper bound of the slew rate of the inputs

$a_1(k)$ Soft constraint used to avoid the vehicle get close to the margins of the road and other vehicles

e_y^{max} Maximal lateral error respect to the center of the road allowed

e_y^{min} Minimal lateral error respect to the center of the road allowed

H_p Prediction horizon

L Linear term of the objective function associated to the state values

P Linear term of the objective function associated to the soft constraint $a_1(k)$

Q Quadratic term of the objective function associated to the state values

R Quadratic term of the objective function associated to the inputs

S Linear term of the objective function associated to the progression of state s

U Set of all input variables at all time instants evaluated at the objective function

u_{min}, u_{max} Lower and upper bound of the inputs

x_{min}, x_{max} Lower and upper bound of the states

Kinematic and Dynamic Model Notation

$\Delta\delta$ Variation of the steering angle

δ Steering angle

κ Curvature of the road

μ Friction coefficient

ω Angular velocity defined with respect to the robots reference frame

θ_e Angular error respect to the curvature of the road

a rear wheel acceleration

C_f Front tire stiffness coefficient

C_r Roar tire stiffness coefficient

e_y Lateral error respect to the center of the road

I Vehicle yaw inertia

l_f Distance from center of mass to front wheel

l_r Distance from center of mass to rear wheel

m Mass of the vehicle

s Distance travelled according to the map

v_x Longitudinal velocity defined with respect to the robots reference frame

v_y Lateral velocity defined with respect to the robots reference frame

State-Space Representation Notation

A Matrix used at state-space representations associated to the influence of current state values over the systems dynamics

A_{ij} Dynamic term of matrix A which related the influence of state j over state i

B Matrix used at state-space representations associated to the influence of inputs over the systems dynamics

B^+ Pseudo-inverse of matrix B

T_s Sampling time for discretization

$u(t)$ Set of all inputs of the model at a determined time instant t

$x(t)$ Set of all states of the model at a determined time instant t

Sets Notation

$\hat{S}_u^k$ Provisional zonotope with a determined set of inputs computed for a determined time instant k

$\hat{S}_x^k$ Provisional zonotope with a determined set of states computed for a determined time instant k

S_u^C Zonotope with the lower and upper bound of the inputs

S_u^k Zonotope with a determined set of inputs computed for a determined time instant k

$S_x^{C_k}$ Zonotope with the lower and upper bound of the states for a determined time instant k

S_x^k Zonotope with a determined set of states computed for a determined time instant k

$S_{\Delta u}$ Zonotope with the maximal and minimal increment of the inputs allowed

Chapter 1

Introduction

This first chapter aims to help the reader to get into the master's thesis by exposing the historical context in which it has been developed, describing the personal motivation that encouraged the author to develop it as well as exposing the objectives of the project and a description of the structure of this document.

1.1 Motivation

The world is currently in a critical situation in which society must rethink different crucial aspects related to energy management and mobility due to the energy crisis as consequence of the war in Ukraine and the climate emergency that our planet is suffering.
Among the main challenges facing today's society one of the most important is the necessity of transitioning from the current model to a new model of sustainable mobility.

Regarding the technological context, we are currently living in a continuous revolution where year after year the existing technologies are being improved, allowing more complex calculations in lower computational time.
At the same time, communications are in constant development improving the communication speed between devices and its efficiency through new communication protocols with low latency.
There are many experts who highlight the importance of these two concepts and point to 5G technology as one of the cornerstones to achieve more connected cities that implies a more coordinated and a more sustainable transport management [9].

Despite mobility is only one of the aspects to be improved in our society, many experts show the

great positive impact for the environment that reducing traffic would entail thanks to efficient coordination between the different vehicles [6], [13], Also transport based on well coordinated autonomous vehicles is expected to improve the quality of life of the users as well as increase the safety and security of mobility reducing the number of traffic accidents [28].

To improve the safety and the efficiency of transportation, many aspects are being studied such as solving control, communication and sensing challenges related with the coordination problem of autonomous vehicles [11]. Of all the aspects that have to be dealt with on the field of safety coordination, this master's thesis is focused on the study of path planning techniques for autonomous vehicles based on optimization criteria.

1.2 Objective

The main objective of this project is to analyse the state of the art in the field of safety coordination of autonomous vehicles and study, develop and compare different techniques focused on optimizing the traffic,considering comfortable manoeuvres and increasing the safety of the passengers from the point of view of path planning avoiding fixed and mobile obstacles .
For this purpose, the results of different optimization-based planners based on MPC techniques have been developed and compared, using both kinematic and dynamic models. Resolutions based on nonlinear systems and linear systems using LPV techniques have been proposed.
In addition, it has been considered that the main component of the optimization criteria should be the safety of the passenger and other vehicles, for which different ways of including obstacle avoidance have been studied such as introducing set-theory to delimit the problem to viable regions based on safety criteria. A more detailed reasoning of its relevance is given in the following chapter.

1.3 Research Frame

The development of this TFM is framed under the research project "Safe and Secure Coordination of Autonomous Vehicles (SaCoAV)" (ref. MINECO PID2020-114244RB-I00) which is co-financed by the Spanish State Research Agency (AEI) and the European Regional Development Fund (ERFD).
The aim of the SaCoAV project is to extend the research developed in a previous project called "Safety and Control in Autonomous Vehicles (SCAV)" to a scenario with multiple vehicles introducing new concepts and aspects of security and safety related with the coordination.

1.4 Structure

This document is divided into the following chapters:

1. **Chapter 1: Introduction.** This chapter presents a small description, the motivation and objectives of the project.

2. **Chapter 2: Theoretical Background.** The aim of the second chapter is to describe the state of the art of the topic and expose different recent research which has been considered while developing this work.

3. **Chapter 3 and 4: Models description.** In these chapters it is described the kinematic and dynamic models which have been used in part of this project. Their main advantages and disadvantages are also discussed.

4. **Chapter 5: Motion planner description.** In this chapter it is described the optimization criteria applied at the different planners developed.

5. **Chapter 6: Implementation.** In this chapter it is detailed the Software and the simulation scenarios used for the different motion planners.

6. **Chapter 7 to 9: Motion planners development.** In these chapters, detailed information of the development and implementation as well as results of each path planner are shown.

7. **Chapter 10: Conclusions and future work.** In this last chapter it is discussed the results obtained after describing and comparing the different techniques developed. Also future work to continue this project is proposed.

8. **Appendix.** At the appendices the time planning, economical budget and the environmental and social impact study have been presented.

Chapter 2

Theoretical Background

The aim of this chapter is to present the state of the art of the topic at the moment this work has been developed to understand the starting point of this project and how it has been focused.

2.1 Autonomous Vehicles

As mentioned at [32], autonomous vehicles are those vehicles which can be considered as part of the ITS (Intelligent Transportation System) having increasingly more capability to drive without the intervention of a human decreasing number of accidents and traffic jams while improving the safety and comfort of the users.
They are also known as driverless or self-driving vehicles and can be classified according to different criteria. This section evaluates two of them, the levels of autonomy and its communication system.

2.1.1 Levels of Autonomy

The most extended classification of vehicles according to its autonomy is the levels of autonomy proposed by the SAE International (Society of Automotive Engineers) and NHTSA (U.S. Department of Transportation's National Highway Traffic Safety Administration) under the Standard J3016. As explained at [31], 6 levels of autonomy are considered:

- **Level 0**: No automation available.
- **Level 1**: The driver control almost everything but some components may be performed automatically.
- **Level 2**: The driver controls the vehicle but counts with some assistance.

- **Level 3**: At this point, the car may work automatically being supervised by the driver. Sometimes the controller may ask for human intervention.
- **Level 4**: It is the first level of autonomy where the autonomous driving without human intervention is guaranteed. It is considered level 4 if it works only for specific scenarios.
- **Level 5**: This level is the corresponded to a fully automated vehicle. The autonomous vehicle works without human intervention at every possible scenario.

2.1.2 Communication

As mention in the previous chapter, another key element of this technology is the use of the 5G standard, because the communication plays an important roll in the automation process. Therefore, other classifications based on the type of coordination could be performed as the proposed at [11]:

- **V2V Communication**: Communication between cars. A vehicle receives and sends information to the vehicles around it. It is also known as inter-vehicle communication (IVC).
- **V2I Communication**: Communication between the car and the infrastructure. A supervisor collects information from the vehicles and has the task of supervising and managing the coordination of vehicles. There is a wide sort of proposals for the coordinator. It is also known as road-side to vehicle communication (RVC).
- **V2X Communication**: The X makes reference to "everything", that means, not only infrastructure and other vehicles are communicated with it, other entities such as devices, pedestrians or bicycles are also communicated.

Depending on the agents implicated in the communication, different protocols and technologies are used according to the range and latency needed [31].

2.2 The Coordination Problem

Many aspects of autonomous vehicles have to be improved like perception or develop from new smart infrastructures but this project is centered in another aspect which is the coordination of vehicles.
As it is described at the article [11], the main difficulties appear when different vehicles have to share common resources like roundabouts or intersections. Thanks to the V2V or V2I vehicles

communication, there exists a wide range of possibilities for designing new criteria to coordinate them more efficient than traditional coordination systems such as traffic lights or traffic signs.

2.2.1 Main Challenges

As the mentioned article proposes, all new ideas should be focused on improving the performance while guaranteeing safety and liveness constraints. Accordingly, new challenges to be taken into account have to be faced which are the sensor uncertainties, the imperfection of communications and the necessity of avoiding collisions, which also means computing feasible solutions guaranteeing safety constraints keeping the vehicle away from positions where future collisions are not avoidable.

2.2.2 Solutions

The article [11] classifies the different proposals in two groups:

- **Rule-based solutions**: These solutions make reference to those whose coordination is managed by an external system in charge of coordinating vehicles following a determined rule like prioritizing the longest queue on an intersection or a first-come-first methodology. Many of those techniques are discussed at [30]. As the authors of [11] say, these techniques are suitable from the computational and economical point of view, but may not capitalise all the strengths and opportunities provided by coordinated autonomous vehicles.

- **Optimization-based solutions**: These proposals make a mathematical formulation of the problem solving it using algorithms from optimal automatic control such as MPC or time receding horizon control. As explained at [11], this formulation allow the designer to split the problem into feasibility and optimality guaranteeing safety and the best performance under the desired criteria. On the other hand, the computational cost is higher, but it could be divided in different sub-problems combining centralized and decentralized optimal problems. An example of centralized optimization-based solution is the proposed at [20] where a centralized system tries to determine the reference speed of each vehicle on an intersection to avoid collisions while optimizing the global time needed to cross. While many others decentralized approaches have been proposed like the defined at [30] which suggest an ego-based coordination where every vehicle computes its optimal action by itself under its own performance and safety criteria gridding the intersection and communicating others the desired cells reducing or accelerating when overlaps are predicted to avoid collisions.

2.3 Optimization-based Motion Planning

To reach the objectives of this project, optimization-based solutions for the coordination problem are considered. The liveness and safety problem is regularly addressed from two different perspectives. Both of them consist in two differentiated parts, the path planner which generates a reference and a control whose aim is to follow the reference provided by the planner:

- A first approach generate a basic path according to a performance criterion and a powerful motion control adjust the movements of the vehicle not only to follow the reference as much as possible, but also to include safety and liveness condition inside the problem. That is, the motion controller is the responsible of avoiding obstacles and guaranteeing the safety of the passengers.
- Meanwhile, the second approach emphasize in designing a complete path using a motion planner (MP) which takes into account, not only the performance of the vehicle, but also the liveness and safety constraints, guaranteeing the integrity of the vehicle and the passengers independently on the accuracy of the motion controller implemented on the vehicle.

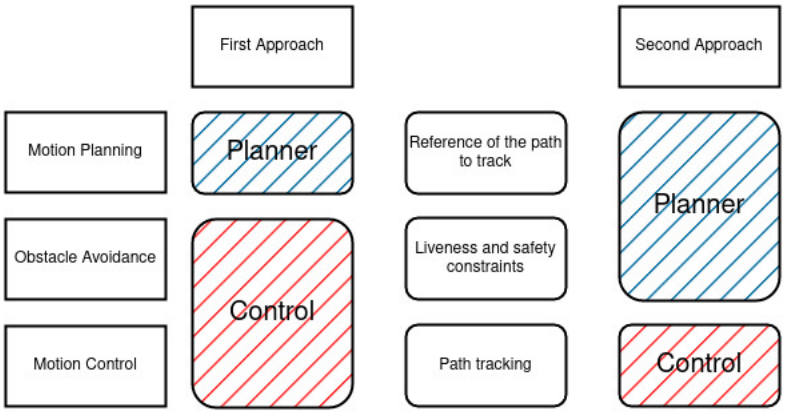

Figure 2.1: Approaches to cover obstacles avoidance.

The first approach allow the system to compute the path with a higher prediction horizon or with a wider sampling time, while the effort and the response capability of the motion controller have to be powerful enough to guarantee specifications.
On the other side, the motion controller can be more basic if the motion planner is accurate or complex enough to consider the uncertainties of the system and design paths which guarantee

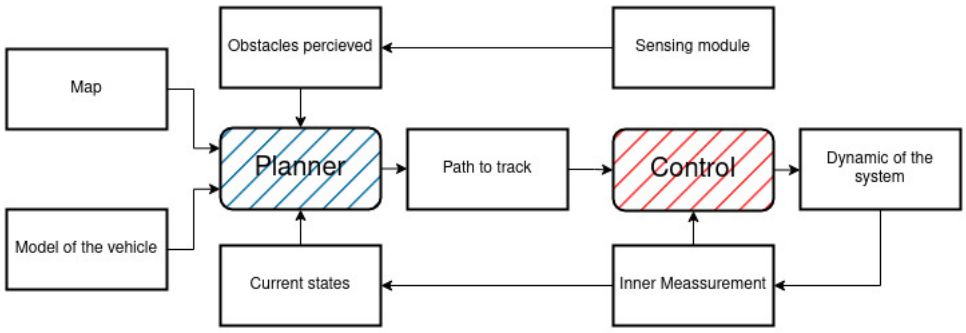

Figure 2.2: Scheme of the planner-control interaction.

that the vehicle will not reach a state where a future collision is unavoidable.
The second solution reacquires a more complex statement of the planner what also implies a higher computational cost. Therefore, complementary techniques to simplify the computation have to be considered.
This project is focused on the planner of the second approach resulting in a scheme as the shown at Figure 2.2.

2.4 Motion Planner Techniques

As mentioned above, there exists a promising line of research of our interest focused on motion planning based on optimization techniques such as MPC. Theoretical studies typically use non-linear models as at [12] but as it is mentioned at the article, the computational effort play an important role when designing motion planners based on MPC techniques. Hence, other articles which achieve reduced computational time reduction without forgetting the importance of uncertainties has been studied.

2.4.1 Inclusion of LPV Techniques

Modelling a system using LPV techniques consists in representing systems with non-linearities skipping linearizations around operational-points using a state-space representation which considers the variation of some parameters [29]. The matrices of the system can be defined as a linear combination of a set of linear matrices weighted according to some gains that have the non-linearities of the system embedded. Another option, which is the followed at this work, is to compute linear matrices to represent the system at each iteration.
As a noticeable advantage, avoiding the use of non-linear system allow the formulation of the problem as a convex linear one which can be easily solved with common used tools such as

those specifically designed for MPCs. Furthermore, uncertainties introduced by linearizations are avoided.
The article [3] present a motion planner using LPVs matrices (LPV-MP) while propose a protocol to avoid static obstacles based on defining a security area around it at modifying the constraints of the optimization problem according to it. Both aspects, the use of LPVs and the obstacle avoidance criterion, are very interesting and considered for this project.

2.4.2 Inclusion of Set-Theory

Another interesting aspect is the inclusion of concepts belonging to set theory which is an interesting manner of designing robust system based on defining sets or kernels of states or inputs which guarantee some desired constraints. Some useful concepts explained at [33] should be remarked to understand why it is relevant and should be considered in motion planners:

- Invariance kernel: set of dynamic states that guarantee remaining inside a determined set of constraints for all times.
- Viability kernel: All dynamic evolution of the states belonging to this set will comply the constraints in a determined time horizon.
- Capture basin: a state belongs to the capture basin of a region C (subset o the constrained set) if any of its possible evolution reach C in a finite time period.
- Forward maximal reachable set: Starting with an initial set of state, the forward maximal reachable set at a specific time instant t are all possible states to which the system can evolve considering all possible inputs.
- Backward maximal reachable set: Inversely, the backward set are all the initial states which could have evolve to a specific set at a determined time instant.
- Tube: Time propagation of a set.

As explained at [33], those concepts can be used to certify the safety of a system. Analyzing possible disturbances, it can be determined the set of states or inputs which guarantee the system remain inside the safety region defined by numerical constraints, it can be used also to guarantee some performance specifications.
There are very powerful tools which have been applied to motion planning in recent articles like [8], article which proposes the use of invariant sets to track a reference avoiding the obstacles, but making use of linearized models. Likewise, other works like [17] ensure having reduced computational time of complex coordination situations introducing reachability analysis to the

reduce the complexity optimization problem while increasing the robustness of the planner. This proposal is based on defining safety corridors using a simplified and linearized model of a vehicle to avoid non-linearities.

As it can be observed, those proposals do not include LPV concepts to reduce the computational time and the uncertainties of disturbances proposed at [33] for other research fields.
The computation of sets and operations between them like intersections to prove safety, may also introduce more computational cost, therefore, different alternatives have been studied like assuming the resulting tube convex and finding the limits computing trajectories as in [15], but other alternatives can be used like under-approximating the kernels by zonotopes as proposed at [21].
Zonotopes are a type of set which can be defined by the center and a matrix generator with basic operational tools as explained at [2] and can be easily used to compute a tube of states propagating the dynamic of the system described, even if the dynamic of the system is non-linear, a zonotope can be used to approximate the tube as the viability kernels computed at [7].

As it has been proved, researchers already have start using set-theory for motion planners while LPV techniques are used to simplify the complexity without loosing properties, but just few scientific studies like [4] combine both. This work proposes the control of an autonomous vehicle using an MPC avoiding linearizations using an LPV representation of the dynamic of the vehicle and guarantee safety thanks to a reachability analysis using zonotopes.

2.5 Contribution

Once the main aspects discussed along this project have been presented, it has been evidenced that many aspects have to be covered to achieve level 5 of autonomy of vehicles. Focusing on V2V communicated vehicles, it can be seen how wide is the field of safety coordination based on motion planners and its potential, being many research lines still open.
During this document it will be discussed the possibility of designing a novel motion planner using LPV techniques combined with zonotopic tube-based reachability analysis inspired in the zonotopic tube-based LPV-MPC controller presented at [4] while integrating LPV techniques and obstacle avoidance protocols inspired in the motion planner described at [3], but going further thanks to set-theory and including movable obstacles assuming the autonomous vehicle counts with V2V or V2X communication.

Chapter 3

Kinematic Model Description

The aim of this chapter is to describe the first vehicle model used and the path planner developed based on it.

3.1 Non linear Kinematic Representation

The first representation studied is a curve-based kinematic model [5] based on the classical bicycle model [24] which has been proved its functionality when planning feasible trajectories [23]. This alternative representation based on the curvature of the map was presented at [1]. It consists in five states: linear velocity ($v(t)$), steering angle ($\delta(t)$), the distance to the closest point to an imaginary curve located at the center of the road (e_y),the difference of orientation between the mentioned imaginary curve and the vehicle ($\theta_e(t)$) and the distance travelled measured making a projection of the current position of the vehicle over the imaginary curve ($s(t)$). As inputs of the system the linear acceleration $a(t)$ is considered as well as the variation of the steering angle $\Delta\delta(t)$.

Among this document, the states $e_y(t)$ and $\theta_e(t)$ are also called lateral and angular error to preserve the habitual nomenclature used in the literature where those states are typically used based on the path to follow instead of the center of the road.

As it can be observed in the equations (3.1) to (3.6), also other parameters play a roll in the dynamic evolution of the system which are the curvature of the road κ based on the map described by the imaginary curve already mentioned, the dimensions of the vehicle being l_r and l_f the distance from the point of the vehicle studied to the rear and front part of the vehicle, and also an angular measure formulated as $\beta(t)$ which is just a magnitude formulated to simplify the equations.

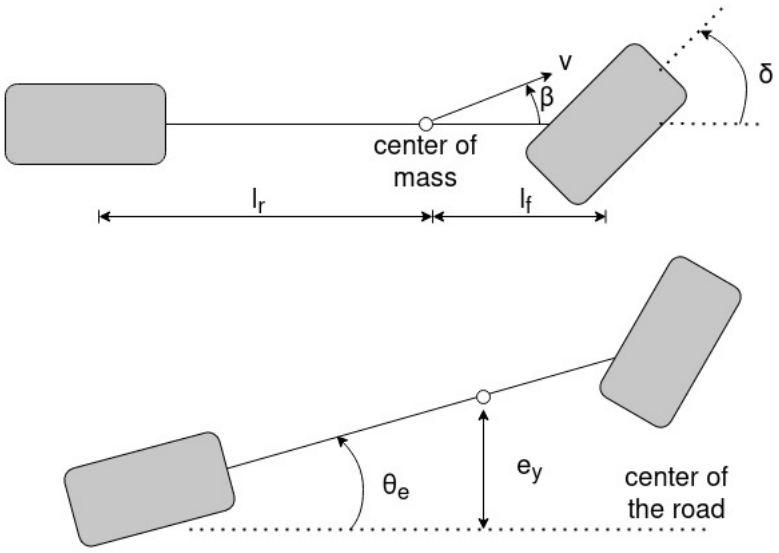

Figure 3.1: Vehicle model: Relevant states and variables.

Additionally, it is also important to remark that the state $s(t)$ can be excluded from the dynamic model because its dynamic is affected by other states but it does not modify the values of the others. It has been included because its magnitude is very useful to locate the vehicle over the map and evaluate if a path planned consider a big displacement or not, but it could be computed in parallel to the dynamic system in case controllability problems occurred.

$$\dot{v}(t) = a(t) \tag{3.1}$$

$$\dot{\delta}(t) = \Delta\delta(t) \tag{3.2}$$

$$\dot{e_y}(t) = v(t)cos\left(\beta(t)\right) sin(\theta_e(t)) + v(t)sin\left(\beta(t)\right) cos(\theta_e(t)) \tag{3.3}$$

$$\dot{\theta}_e(t) = v(t)\frac{sin(\beta(t))}{l_r} - v(t)\frac{cos\left(\beta(t)\right) - sin\left(\beta(t)\right)}{1 - e_y(t)\kappa}\kappa \tag{3.4}$$

$$\dot{s}(t) = v(t)\frac{cos(\beta(t)) - sin(\beta(t))}{1 - e_y(t)\kappa} \tag{3.5}$$

$$\beta(t) = \arctan\left(tan(\delta(t))\frac{l_r}{l_r + l_f}\right) \tag{3.6}$$

3.1.1 Discretization

The system has been discretized following the rule $x(k+1) = x(k) + T_s \cdot \dot{x}(k)$.
The use of $\Delta\delta(t)$ as input of the system is useful to obtain a more realistic model of the vehicle

because the steering angle of the vehicle can not vary instantly, but when discretizing the system, depending on the magnitude of the sampling time and the range of the steering angle, the model can be easily modified to considers the steering angle as the input instead of its slew rate.

3.1.2 Main Advantages and Disadvantages

The main advantage of this model is its simplicity describing the kinematic of a vehicle with four states in case of using the version which use the second state ($\delta(t)$) as the input of the system.
On the other hand, the non-linearities introduce computational complexity for the optimization problem or error if the system is linearized around an operational point. A good manner to partially solve this problematic is to locate the point studied at the front wheel of the bicycle model, identifying the parameter $\beta(t)$ (3.6) as $\delta(t)$.
Additionally, it is also important to remark its high dependency to the linear velocity blocking the model when its value gets zero, or the same problematic when angle $\beta(t)$ is null, obtaining a non-controllable system.
For those reasons, it is not desirable to make use of the kinematic model in the path planner out of non-linear optimization problems.

Chapter 4

Dynamic Model Description

The aim of this chapter is to present the second vehicle model used to solve the controllability problematic and the path planner developed based on it.

4.1 Non Linear Dynamic Model

This second model also known as curvature-based nonlinear model of a bicycle is not independent from the previously described at Chapter 3, but a more realistic one after having introduced new terms related with the dynamic of the vehicle as described in details at [5].
As it main advantages, its complexity allows obtaining more realistic simulations, however, increasing the complexity is translated into higher computational costs and big errors if the dynamic parameters are not well estimated.

At this model the inputs considered are the linear acceleration and the steering angle, while the states of the systems are the linear velocity in the direction of the front side of the vehicle ($v_x(t)$), the lateral velocity induced by the dynamic components ($v_y(t)$), the angular velocity ($\omega(t)$) and the previously mentioned lateral error, angular error and distance travelled (e_y(t), θ_e(t) and $s(t)$).

Once again, it can be observed that the sixth state (4.6) can be interpreted as a property of the vehicle and be excluded of the complete model because its dynamics depend on the other five states but it does not interfere in the behaviour of the others.It has been included because it will be used to identify the current position of the vehicle over the map and the distance travelled by the vehicle in a certain period of time.

$$\dot{v}_x(t) = a(t) - C_f \frac{\delta(t) sin(\delta(t))}{m} + \omega(t) v_y(t) - \mu v_x(t) + C_f sin(\delta(t)) \frac{\omega(t) l_f + v_y(t)}{m v_x(t)} \tag{4.1}$$

$$\dot{v}_y(t) = C_f \frac{\delta(t) cos(\delta(t))}{m} - v_x(t)\omega(t) - v_y(t) \frac{C_r + C_f cos(\delta(t))}{v_x(t) m} - \omega(t) \frac{C_f l_f cos(\delta(t)) - C_r l_r}{v_x(t) m} \tag{4.2}$$

$$\dot{\omega}(t) = C_f \frac{\delta(t) cos(\delta(t)) l_f}{I} - v_y(t) \frac{C_f cos(\delta(t)) l_f - l_r C_r}{v_x(t) I} - \omega(t) \frac{C_f cos(\delta(t)) {l_f}^2 + C_r {l_r}^2}{v_x(t) I} \tag{4.3}$$

$$\dot{e}_y = v_x(t) sin(\theta_e(t)) + v_y(t) cos(\theta_e(t)) \tag{4.4}$$

$$\dot{\theta}_e(t) = \omega(t) + \kappa \frac{v_y(t) sin(\theta_e(t)) - v_x(t) cos(\theta_e(t))}{1 - e_y(t)\kappa} \tag{4.5}$$

$$\dot{s}(t) = \frac{v_x(t) cos(\theta_e(t)) - v_y(t) sin(\theta_e(t)))}{1 - e_y(t)\kappa} \tag{4.6}$$

Comparing the dynamic model with the kinematic model studied, new terms and parameters are introduced such as the mass of the vehicle (m), an auxiliary coefficient to group all friction and independent terms (μ), the vehicle yaw inertia (I) and the rear and front tire stiffness coefficient (C_r and C_f).

4.2 Discretization and LPV State-Space Representation

The system has been discretized following the same discretization approaches as used with the kinematic model at Chapter 3 which consist in computing the value of next state as $x(k+1) = x(k) + T_s \cdot \dot{x}(k)$.

Analyzing equations (4.1) to (4.6), it is observable that the development of a state-space representation must deal with many non-linearities and time-varying parameters such as sinus and cosinus of input $\delta(t)$ and the state $\theta_e(t)$ or external parameters like the curvature of the road at the point where the vehicle is located at each time instant.
For this reason, it has been selected an LPV representation of the system whose magnitudes depends on the values of the each state at the previous time instant, the input applied, and the curvature of the road. By this way, the error inferred by this approach is considerably lower than the introduced by a linearization of the system, allowing to obtain more realistic results but obtaining a higher computational time caused by the introduction of a new step to compute the LPV matrices used at the optimization problem.

4.2.1 Controllability

The controllability of a system can be defined as the capability to drive each state of the system to a specific desired value in a finite time period. As it was commented at Chapter 3 , it was not reachable linearizing or using an LPV state-space representation of the kinematic model. Trying to avoid those problems, some approaches have been applied in order to get a fully controllable system representation by decomposing each equation in many different terms avoiding an LPV representation whose states do not show the real inter-dependency of each states with the others.

4.2.1.1 Approaches Applied

$$sin(\theta_e(t)) = \frac{sin(\theta_e(t))}{2} + \frac{sin(\theta_e(t))}{2} \simeq \frac{sin(\theta_e(t))}{2} + \frac{\theta_e(t)}{2} \tag{4.7}$$

$$cos\,(\theta_e(t)) = \frac{cos(\theta_e(t))}{2} + \frac{cos(\theta_e(t))}{2} \simeq \frac{cos(\theta_e(t))}{2} + \frac{1}{2} \tag{4.8}$$

Those approaches can be applied because the maximal relative error induced working inside the interval $\theta_e(t) \in [-0,36, 0,36]$ are $1,097\%$ at approach (4.7) and $3,425\%$ at approach (4.8).

4.2.2 LPV Matrices

The state-space LPV representation of the curvature-based dynamic model of a two wheels bicycle used has the structure $\dot{x}(t) = A(t)x(t) + B(t)u(t)$ being $u(t) = [a(t), \delta(t)]^T$ and $x(t) = [v_x(t), v_y(t), \omega(t), e_y(t), \theta_e(t), s(t)]^T$ respectively while matrices $A(t)$ and $B(t)$ are the LPV matrices calculated at each time instant depending on the current values of the inputs and states.

$$B(t) = \begin{bmatrix} 1 & -C_f\frac{sin(\delta(t))}{m} \\ 0 & -C_f\frac{cos(\delta(t))}{m} \\ 0 & C_f\frac{l_f cos(\delta(t))}{I} \\ 0 & 0 \\ 0 & 0 \\ 0 & 0 \end{bmatrix} \tag{4.9}$$

$$A(t) = \begin{bmatrix} 0 & C_f\frac{sin(\delta(t))}{v_x(t)m} & A_{13}(t) & 0 & 0 & 0 \\ -\omega(t) & A_{22}(t) & A_{23}(t) & 0 & 0 & 0 \\ 0 & A_{32}(t) & A_{33}(t) & A_{34}(t) & 0 & 0 \\ \frac{sin(\theta_e(t)}{2} & cos(\theta_e(t)) & 0 & 0 & \frac{v_x(t)}{2} & 0 \\ -\kappa\frac{cos(\theta_e(t))}{1-e_y(t)\kappa} & \frac{\kappa sin(\theta_e(t))}{2-2e_y(t)\kappa} & 1 & 0 & \frac{\kappa v_y(t)}{2-2e_y(t)\kappa} & 0 \\ \frac{cos(\theta_e(t))}{1-e_y(t)\kappa} & -\frac{sin(\theta_e(t))}{2-2e_y(t)\kappa} & 0 & 0 & -\frac{v_y(t)}{2-2e_y(t)\kappa} & 0 \end{bmatrix} \tag{4.10}$$

where components A_{13},A_{23}, A_{32}, A_{33} and A_{34} are defined as:

$$A_{13}(t) = v_y(t) + C_f\frac{l_f sin(\delta(t))}{v_x(t)m} \tag{4.11}$$

$$A_{22}(t) = -\frac{C_r + C_f cos(\delta(t))}{v_x(t)m} \tag{4.12}$$

$$A_{23}(t) = \frac{C_r l_r - C_f l_f cos(\delta(t))}{v_x(t)m} \tag{4.13}$$

$$A_{32}(t) = -\frac{C_f l_f cos(\delta(t)) + C_r l_r}{I v_x(t)} \tag{4.14}$$

$$A_{33}(t) = -\frac{C_f {l_f}^2 cos(\delta(t)) + C_r {l_r}^2}{I v_x(t)} \tag{4.15}$$

$$A_{34}(t) = -\frac{C_f {l_f}^2 cos(\delta(t)) + C_r {l_r}^2}{I v_x(t)} \tag{4.16}$$

Studying the different terms presents at (4.9) and (4.10) it is observable that the system is fully controllable but there are some situations which have to be avoided or an unstable or uncontrollable system will be obtained.

The most relevant case is the impossibility of working around null velocities, otherwise the magnitude of terms such as (4.11) to (4.16) would tend to infinity. For this reason, the model will be used to describe the evolution of a vehicle driving over a map once it has been started and its linear velocity is not close to zero.

Additionally, it is still important to be aware of the rank of the controllability matrix because some of the terms could be evaluated as zero and the rank condition would not be fulfilled.

Chapter 5

Motion Planner Description

The aim of this chapter is to describe how does the developed optimization-based solution for the coordination problem work, including a description of the optimization criteria for planning a path and the obstacles avoidance methodology.

5.1 MP Approach

The idea of affording the coordination problem via a motion planner is to find a feasible trajectory to follow which guarantees the safety of passengers and the integrity of the vehicle. The trajectory get defined as a time distributed sequence of desired states that the controller will use as reference. There are two approaches to ensure a safe driving: One of them consists in computing a basic trajectory and later apply a robust controller which adjusts the movements of the vehicle to follow as much as possible the predefined trajectory but applying safety criteria, the other option, which is the approach selected for this work, consists in designing a more complex, but robust, trajectory with safety mechanisms integrated such as obstacle avoidance ensuring that the autonomous vehicle will act safely with a controller whose unique aim is to follow the robust path.

5.2 Cost Function Definition

A good manner to ensure the safety mentioned above is limiting the control action and the state values according to physical limitations and safety reasons such as the allowed lateral error ($e_y(t)$) according to the road and the obstacles positions.

Furthermore, it is important to reward high velocities and advances along the road in order to obtain efficient trajectories understanding as positive reaching the goal as fast as possible avoiding traffic jams. To achieve more efficient trajectories, the longitudinal location of the vehicle is not relevant, but it is penalizing in case the vehicle gets close to the limits of the road or an obstacle.
Additionally it is interesting to penalize big changes in the steering angle and the acceleration in order to obtain smoother trajectories which also mean more comfortable trips for passengers. Those objectives have been formulated as a quadratic objective function to be minimized. It works as a typical MPC problem being useful the specific tools developed for them.

$$\begin{aligned}\arg\min_{U} \sum_{k=1}^{H_p} \left[P a_1(k)^2 + x(k)^T Q x(k) + L x(k) \right] + S\left[s(H_p) - s(0)\right] + \\ + \sum_{k=0}^{H_p-1} \begin{bmatrix} u(k)^T & \Delta u(k)^T \end{bmatrix} R \begin{bmatrix} u(k) \\ \Delta u(k) \end{bmatrix}\end{aligned} \tag{5.1}$$

subject to:

$$U = [u(0), ..., u(H_p - 1)] \tag{5.2}$$

$$x_{min}(k) \leq x(k) \leq x_{max}(k) \tag{5.3}$$

$$u_{min}(k) \leq u(k) \leq u_{max}(k) \tag{5.4}$$

$$\Delta u_{min} \leq \Delta u(k) \leq \Delta u_{max} \tag{5.5}$$

$$0 \leq a_1(k) \leq 1 \tag{5.6}$$

$$-2 + 3\frac{e_y(k)}{e_y^{min}(k)} \leq a_1(k) \tag{5.7}$$

$$-2 + 3\frac{e_y(k)}{e_y^{max}} \leq a_1(k) \tag{5.8}$$

In case of a non-linear optimization problem:

$$x(k+1) = x(k) + T_s \dot{x}(k) \tag{5.9}$$

being $\dot{x}(k)$ the non-linear differential equation which describes the dynamic of the system at a certain time instant k.
In case of linearizing around an operating point or describing the system with LPVs techniques,

the problem gets quadratic:

$$x(k+1) = A(k)x(k) + B(k)u(k) \tag{5.10}$$

Terms L and Q are associated to the states by rewarding high velocities and penalizing big magnitudes of undesirable states like big angular velocities, wide lateral or angular errors avoiding the trajectory get close to a non-feasible region.
Matrix R is the responsible of obtaining a smooth trajectory penalizing aggressive maneuvers, and S reward progress in the road.

Matrix P is used as a soft constraint penalizing the vehicle when it is located closer to an obstacle or the limits of the road than to the center, because equations (5.6) to (5.8) constraint the auxiliary parameter $a_1(k)$ which will value zero if the distance of the vehicle to the center of the road is lower than the double of the distance to the lateral limit of the road or the closest obstacle and will get a higher value between zero and one the closer it gets to the maximal lateral error allowed.

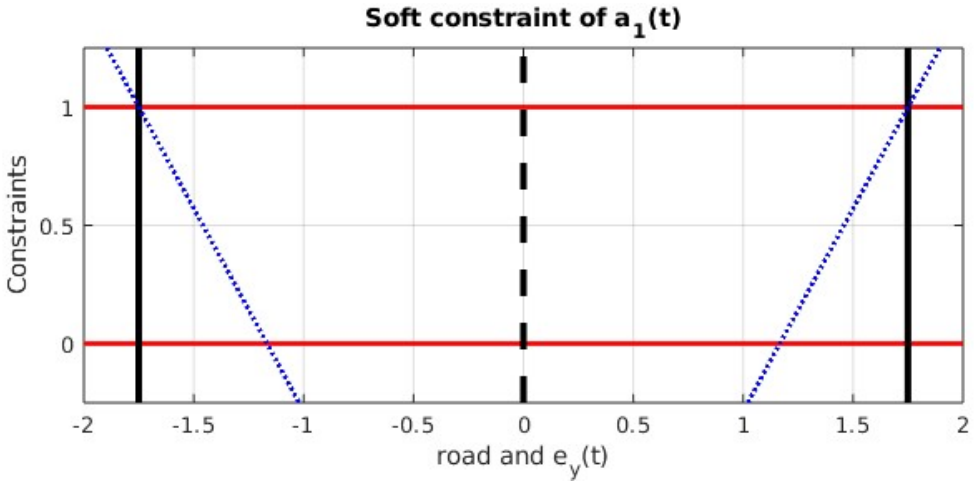

Figure 5.1: Inequalities of the soft constraint $a_1(k)$

It can be easily understood observing Figure 5.1. The discontinuous black line shows the center of the road, while the straight ones show the limits of it, inequality (5.3) force the vehicle to be located inside this band. The red lines represent inequality (5.6), while the blue lines represent inequalities (5.7) and (5.8). The feasible region of $a_1(k)$ is delimited inside the polygon defined by the red band and the blue lines, being the minimal value of $a_1(k)$ 0 if it is in the 75% of the road closest to the center, penalizing the location of the vehicle only if it is

very close to the road limits (or an obstacle).

5.3 Constraints and Limitations

The constraints presented from (5.3) to (5.10) have to be selected according to the physical limitations of the system like maximal accelerations and steering angle or according to security issues such us the maximal angular velocity or the angular error.
Furthermore, one of the most important constraints of the problem is the maximal lateral error allowed ($e_y(t)$) to ensure driving always over the road and avoid collisions with any static or moving obstacles such as pedestrians or other vehicles. At this problem it is assumed that the physiognomy of the road is known having knowledge of the curvature (κ), width and center of the road at any moment. This allows us to use the curvature-based model of the vehicle analyzing its location as its projection over the center of the road ($s(t)$), its orientation compared with the curvature of it via ($\theta_e(t)$) and the distance from the center of mass of the vehicle to the center of the road ($e_y(t)$).

Additionally, a posterior step has to be included to reduce the maximal lateral error permitted not only based on the road width but also on the location of obstacles.

5.4 Obstacle Avoidance

At this problem it is considered that the vehicle has integrated communication devices and an advanced perception system embedded which provide the planner, the position of obstacles over the road and an estimation of their evolution in future steps. For this project only stopped and driving vehicles have been considered leaving for future works the inclusion of pedestrians and obstacles whose evolution were unpredictable.

The manner in which $e_y(k)$ has been modified is reducing its value according to the expected position of the vehicle at each time instant based on the path planned in the previous iteration and the expected location of the obstacles at those time instants.

At each iteration of the path planner left and right limits are recomputed according to the most recent path calculated and the newest estimations of how the obstacles are expected to evolve.

This cyclic process has been summarized at Algorithm 1.

The limit computed associated to each obstacle is explained in the following section.

5.4.1 New Lateral Limit Computation

Depending on the position of the obstacle respect to the vehicle, the maximal lateral error is modified according to the Figure 5.2. That is, if the vehicle is located almost at the same position (s) as the obstacle, the maximal lateral error allowed ($e_y(t)$) is reduced to the position of the obstacle minus a safety margin. Choosing a wide enough safety margin allow the process to consider the obstacles as points over the map.

In case the vehicle is located in a forward or backward position this distance (obstacle + safety margin) gets reduced progressively to the road half-width proportionally to the distance between the vehicle and the obstacle.

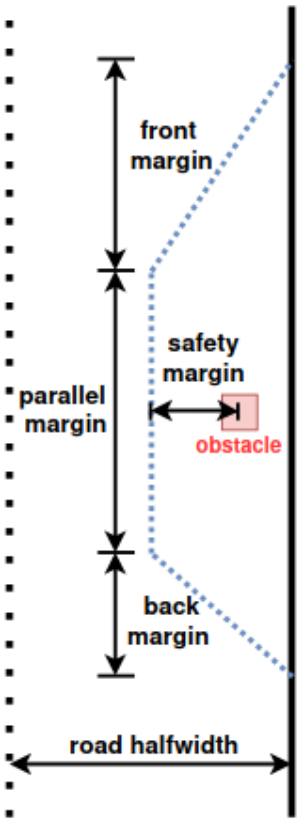

Figure 5.2: Scheme of the lateral limit computation.

5.4.2 Graphical Example

Graphics at Figure 5.3 shows an example where the vehicle (blue) is close to an obstacle (red). The red dots represent the expected position of the vehicle in following time instants, while in green the expected position of the vehicle if the path followed were the computed in previous iteration. The blue curves represent how lateral limits have been reduced along the path according to the expected position of both vehicle and obstacle guaranteeing safety.

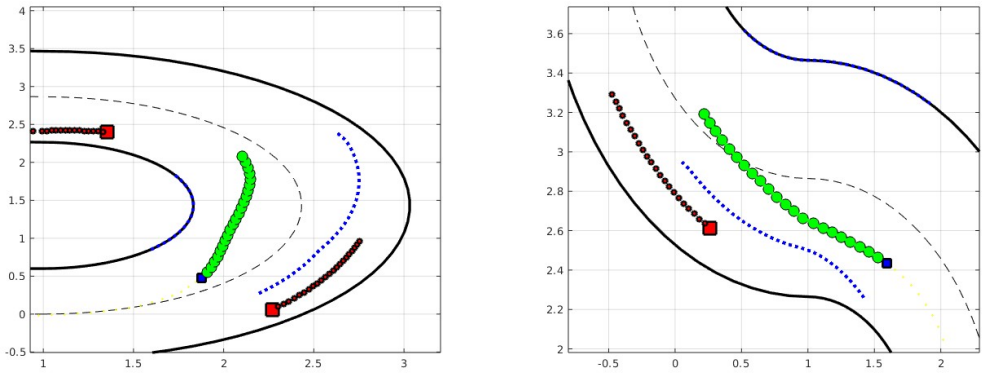

Figure 5.3: Example of lateral limits computed.

Algorithm 1 Determination of lateral limits for obstacle avoidance

Initialization;
path $\leftarrow$ expected $[s_v, e_{y_v}]$ of the vehicle from $k = 1$ to $k = H_p$
Estimation of all positions of all obstacles;
$k \leftarrow 1$
while $k \leq H_p$ **do**
  obs $\leftarrow [s_{ik}, e_{y_{ik}}]$ based on $[s_{ik-1}, e_{y_{ik-1}}]$ and v_i
  list R $\leftarrow$ safety margin computation for each element of **obs** at right side of the road
  list L $\leftarrow$ safety margin computation for each element of **obs** at left side of the road
  $e_y^{max}(k) \leftarrow \min\{\frac{1}{2}roadwidth, \textbf{list R}\}$
  $e_y^{min}(k) \leftarrow \max\{-|\frac{1}{2}roadwidth|, \textbf{list L}\}$
  $k \leftarrow k + 1$
end

5.5 Motion Planners Development

Based on the principles explained at this chapter, different path planners have been developed. On one hand, a non-linear path planner has been designed based on the kinematic model described at Chapter 3 , but its computational cost was undesirable. To improve it, an LPV approach was presented, but due to controllability issues was discarded.
The second manner studied to afford the path planning was making use of the dynamic model. This model allows the use not only of NL solvers but also quadratic ones using LPV approaches as described at Chapter 4.
Furthermore, it has also developed a preliminary version of a path planner which computes the constraints and limitations of the optimization problem introducing set theory (intervals and zonotopes) achieving better results from the computational and safety point of view. More details will be given in following chapters.
To sum up, List5.5 and Algorithm 2 list the path planners developed and summarize the cyclic structure that all o them follow.

- Path planners based on the kinematic model.

  NL-MPC: The computational cost was undesirable.

  LPV-MPC: many unfeasible problems due to be working with a non-fully controllable state-space representation, it was discharged.

- Path planners based on the dynamic model.

  NL-MPC: High computational cost.

  LPV-MPC: Better computational cost and results.

  LPV-MPC with tube propagation: based on sets propagation of the dynamic model.

Algorithm 2 Structure of the path planners developed

Step 1: Read last path planned and obstacles info;
Step 2: Estimate future locations of obstacles;
Step 3: Compute LPV matrices; (Skip if NL-Planner)
Step 4: Compute lateral limits based on obstacles;
Step 5: Determine constraints of the optimization problem;
Step 6: Compute the optimal path with an NL or Quadratic problem;
Step 7: Update variables and parameters;

Chapter 6

Implementation

The aim of this chapter is to explain the implementation of the path planners described in previous chapters.

6.1 Software

The aim of this project is a theoretical study focused on comparing and analyzing different optimization techniques and their advantages and disadvantages. For this reason the simulator and prototypes haven been coded in MATLAB in order to take advantage of all its optimization and graphical toolboxes. The version of MATLAB used is version 9.12.0.1884302 which corresponds to 2022a [18].
Additionally, to simplify and structure the optimization problem, it has been used a commonly used toolbox for rapid prototyping optimization problems called YALMIP.[16].
Furthermore, the set-theory used for the last path planner developed make use of a toolbox called CORA [19], which is a free toolbox focused on continuous reachability analysis, including many classes and functions to handle geometric sets such as zonotopes or intervals.
For being able to run YALMIP and CORA it is necessary to include the Optimization Toolbox, the Symbolic Toolbox and the Multi-parametric Toolbox 3.0 (MPT3) [10] which is free license.

Obviously, once the techniques have been analyzed, the next step would be to implement it in Python using the set of libraries of ROS and test them in a real prototype comparing the theoretical and expected results with practical ones. Until now, everything has been developed just in the theoretical stage.

6.1.1 Solvers

For solving the optimization problems, two different solvers have been used depending of the type of problems. For the non-linear path planners, solver selected has been "fmincon" which is based on gradients and works with nonlinear constraints and objective functions.
For the path planners based in quadratic programming problems solver "Quadprog" has been selected, which is based on and works with quadratic objective functions whose constraints are strictly linear equations. Both are included at the Optimization Toolbox of MATLAB.

6.2 Simulation Scenario

The simulations have been performed using different maps. Those were already developed by previous students and are described as a sequence of curved path sections defined as the length, the curvature and the half of the road width.
Thanks to different methods of the class "map" and some functions adapted from the already coded by previous students, the location of the vehicle can be rapidly calculated using state s to know at which distance from the beginning is the car and the state e_y to know the lateral displacement.
Additionally, static and dynamic obstacles have been distributed over the maps, defining their position by the same states $x_{obs}(t) := [s_{obs}(t), e_{y_{obs}}(t)]$. This definition is suitable for this problem because do not have to be adapted when changing the paths if initial magnitudes s and e_y and their evolution are described as function of the global magnitudes of the map (total length and minimal/maximal road width).
Figures 6.1 to 6.3 show 3 different maps used for testing the different planners developed.

6.2.1 Ground truth of the Vehicle

For testing the algorithms developed, every time a ground truth measure was desired, the car has been simulated defined as a MATLAB ODE45 (ordinary differential equations solver) system using the dynamic equations described at 4 parameterized as described at this chapter. Then, many iterations are planed where the position of the states of the vehicles is read, an optimal path is computed (states and inputs), and the first input of the optimal sequence

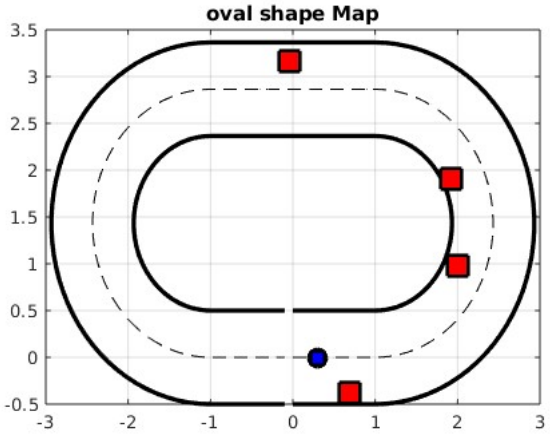

Figure 6.1: Map used for first tests.

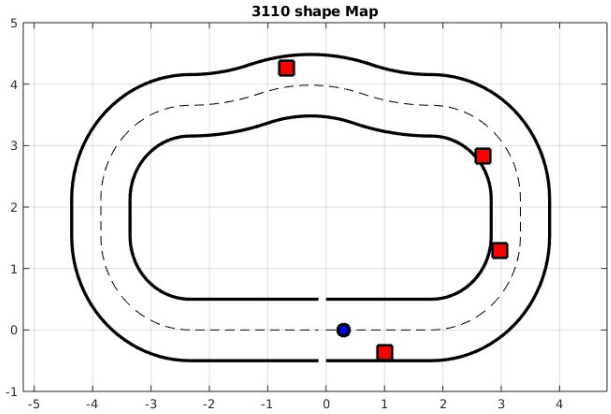

Figure 6.2: Second map used for testing and simulating.

computed is applied to the ODE model.
As future improvement it would be interesting to add some noise to the measurements or to the application of the input or uncertainties of the parameters.

6.3 Structure of the Code

All the codes developed for simulating and testing the different planners follow the same architecture which consists in loading all the elements needed such as the map, the vehicle parameters, the planner used and its constraints, later on an iterative loop is used to simulate a vehicle using the ODE based on the results of the planner, and a final step of saving, processing and

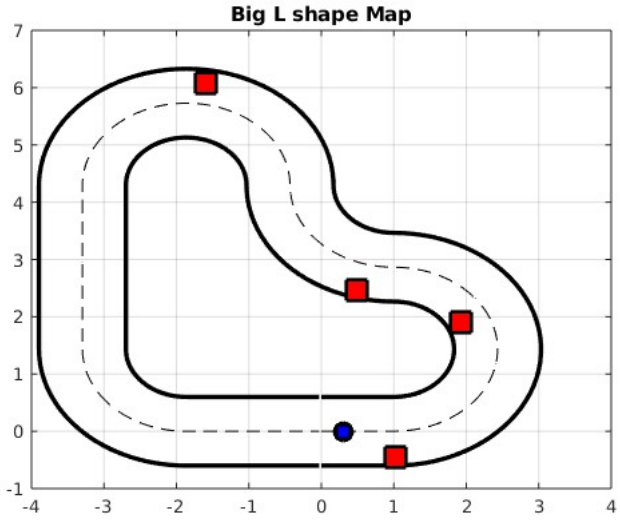

Figure 6.3: Last map used for testing and simulating.

plotting the results obtained. All this process has been summarized at 3.

Algorithm 3 Structure of the testing codes.

Step 1: Definition of the vehicle, map and planner;
Step 2: Initialization of parameters (limits, H_p, number of iterations...);
$k \leftarrow 1$
while $k \leq H_p$ **do**
  Step 3: Read current states of the vehicle;
  Step 4: Execute path planner;
  Step 5: Read the solution provided by the planner;
  Step 6: Simulate the vehicle using the ODE developed;
  Step 7: Save states, path planners and computational time for posterior studies;
  $k \leftarrow k + 1$
end
Step 8: Data processing and plots;

6.4 Parameterization

The parameters of the vehicle have been taken from previous research works developed by previous students.

6.4.1 Parameters of the Vehicle

The dynamic model of the vehicle has been implemented using the parameters present in table 6.1. tables 6.2 and 6.3 show the maximal and minimal values states, inputs and slew rates allowed, which are used as constraints. The states not present at 6.2 are those which are unconstrained (v_y, ω, s), or whose constraints depend on the current position over the map and other obstacles (e_y).

Parameters	Value	Parameters	Value
l_r	0,125 m	l_f	0,125 m
C_r	65 N/rad	C_f	65 N/rad
μ	0,05	I	0,03 kg/m^2
m	1,98 kg		

Table 6.1: Parameters used for the vehicle

Lower bound (states)	Value	Upper bound (states)	Value
${v_x}^{min}$	0,5 m/s	${v_x}^{max}$	2 m/s
ω^{min}	-8 rad/s	ω^{max}	8 rad/s
${\theta_e}^{min}$	-0,5 rad	${\theta_e}^{max}$	0,5 rad

Table 6.2: Upper and lower bounds of states

Lower bound (inputs)	Value	Upper bound (inputs)	Value
a^{min}	-0,103 m/s^2	a^{max}	2 m/s^2
δ^{min}	-0,36 rad	δ^{max}	0,36 rad
Δa^{min}	-80 m/s^3	Δa^{max}	80 m/s^3
$\Delta\delta^{min}$	-13,33 rad/s	$\Delta\delta^{max}$	13,33 rad/s

Table 6.3: Upper and lower bounds of inputs

6.4.2 Parameters of the optimization problem

When designing the objective function, some concepts are very relevant for choosing the values of parameters T_s and H_p.

Choosing a small sampling time reduces the uncertainty introduced by the discretization of the model. On the other hand, for a fixed H_p, the bigger the sampling time is, the longer the path over the time.

Choosing a small prediction horizon reduces the computational time of the objective problem

due to implying complexity reduction of the problem. Meanwhile, the foresight of the vehicle gets reduced for a fixed T_s, delaying the reaction to obstacles or changes in the curvature of the road. In other words, if the planner takes into account a wider distance of the map to the motion design, the trajectory computed will be more efficient.
It is easy to imagine that the ideal case would be to have a T_s close to zero, the larger H_p as possible and a reduced computational time, but that seems unrealistic and not useful. Designing a very large path means solving a very complex problem which frequently is classified as infeasible with the solvers used (even if it is not), and that also means to plan motion in a time horizon that, when reached, the environment will have changed significantly making it useless. Therefore, it is important to find a trade-off between the time horizon ($T_s \cdot H_p$) desired, the accuracy of the solution (T_s), the complexity of the problem (H_p) and obtaining suitable computational time. Also, it is important to consider the performance desired, small T_s with big H_p allows smoother trajectories.
The relevance of this trade-off can be graphically seen at chapter 7 where the influence of both parameters have been discussed comparing different parameterization.

Chapter 7

Non Linear Motion Planners

At this chapter, studies and results obtained from the non-linear motion planners (based on the kinematic and the dynamic problem) are discussed.

7.1 NL Kinematic-Based Motion Planner

The first motion planner (MP) that has been developed was the one based on the non-linear bicycle kinematic model described at Chapter 3 parameterized as in Chapter 6. As mentioned above, for non-convex optimization problems, solver "fmincon" has been used.
This MP has been very useful to analyze the influence of different parameters and to have a first idea of what can be expected from motion planners.

7.1.1 Influence of the Optimization Problem Configuration on Performance

The first concept discussed using the kinematic NL-MP is the need of finding a proper combination of weights. The structure of the matrices used for this study is shown from (7.1) to (7.5).

$$Q = \begin{bmatrix} \frac{q_1}{v_{max}^2} & 0 & 0 & 0 & 0 \\ 0 & 0 & 0 & 0 & 0 \\ 0 & 0 & 0 & 0 & 0 \\ 0 & 0 & 0 & 0 & 0 \\ 0 & 0 & 0 & 0 & 0 \end{bmatrix} \tag{7.1}$$

$$L = \begin{bmatrix} \frac{l_1}{v_{max}} & 0 & 0 & 0 & 0 \end{bmatrix}^T \tag{7.2}$$

$$R = \begin{bmatrix} \frac{r_1}{a_{max}^2} & 0 & 0 & 0 \\ 0 & \frac{r_2}{\Delta\delta_{max}} & 0 & 0 \\ 0 & 0 & 0 & 0 \\ 0 & 0 & 0 & 0 \end{bmatrix} \tag{7.3}$$

$$P = \begin{bmatrix} \frac{p_1}{max - halfwidth^2} \end{bmatrix} \tag{7.4}$$

$$S = \begin{bmatrix} \frac{s_1}{H_p \cdot T_s \cdot v_{max}} \end{bmatrix} \tag{7.5}$$

The idea of Q and L is to potentiate high positive velocities while R penalizes big changes in linear velocity and in the steering angle to obtain a more comfortable performance. Beside that, S and P reward increasing the distance travelled and staying in a safety region of the road, respectively.

7.1.2 Influence of H_p and T_s

For this part of the study,the values selected for matrices (7.1) to (7.5) are the specified at (7.6).

$$q_1 = -\frac{14}{H_p}; l_1 = -\frac{1}{H_p}; r_1 = \frac{400}{H_p}; r_2 = \frac{6219,112}{H_p}; s_1 = -18000 \tag{7.6}$$

The aim of expressing the different weights (7.6) as function of H_p and T_s is to keep the proportional influence of each component of the objective function over the others. For example, if the planner suggests a maximal linear speed among the whole trajectory in a straight path, the proportion between the influence of the velocity and the influence of the progression over the road will be the same independently of T_s and H_p.
The simulation for this study has been performed considering that the motion controller is accurate enough to simplify the algorithm taking the values of the following sates desired according to the planner as the next measures of those states. In other words, it has been considered a perfect motion controller that helps the vehicle to reach the next desired state before re-executing the motion planner.

Five different MP have been simulated and compared to study the influence of H_p and T_s and the proportion between both. Results are shown at Table 7.1 being the two last columns the mean computational time required for each iteration and the progression along the map after a determined number of iterations (30 for T_s 1 second, 60 for 0,05 seconds). The study has been performed using the map "L_shape" and starting at $s = 4{,}2$ meters with an initial linear velocity of 1,5 m/s and a lateral distance to the center of the road of 0,25m. The location has been properly selected to be able to initialize the planner using a realistic vector of predicted curvatures.

As it can be observed, increasing the complexity of the problem by increasing H_p induce an undesired exponential increment of the computational cost of each iteration. Meanwhile, T_s does not affect to the computational cost because the objective function does not change, but if its increment implies an increment of the "temporal length" of the path planned, it has a positive effect. The larger the path, the more efficient the path planned. This effect can be observed comparing scenarios 2 and 3 or 4 and 5, where the computational cost of each pair is around the same value because of having same H_p, but the performance is better in those scenarios with larger paths.
The results of the five simulations have been graphically shown at Figure 7.1. There it can be seen how those with the larger designed path adapt the trajectory better to curvature changes. Additionally, it can be seen how increasing once it is large enough, increasing it from 1 to 2 seconds does not change significantly (Scenario 4 vs 5), therefore, an equilibrium between computational cost and performance has to be found.

	H_p	T_s [s]	$H_p \cdot T_s$ [s]	$T_{compu}[s]$	$\Delta s[m]$
Scenario 1	5	0,1	0,5	0,173108	6,126604
Scenario 2	10	0,05	0,5	0,512454	6,424340
Scenario 3	10	0,1	1	0,515561	6,837890
Scenario 4	20	0,05	1	1,965520	6,424340
Scenario 5	20	0,1	2	1,728516	6,990353

Table 7.1: Results of simulations to study the H_p-T_s trade-off.

Two more simulations using the same configuration as the first (6) and fifth (7) scenario have been performed but using the map "3110" where it can be seen how a larger forecast produces more efficient and smoother trajectories. Those results are shown at Figure 7.2.

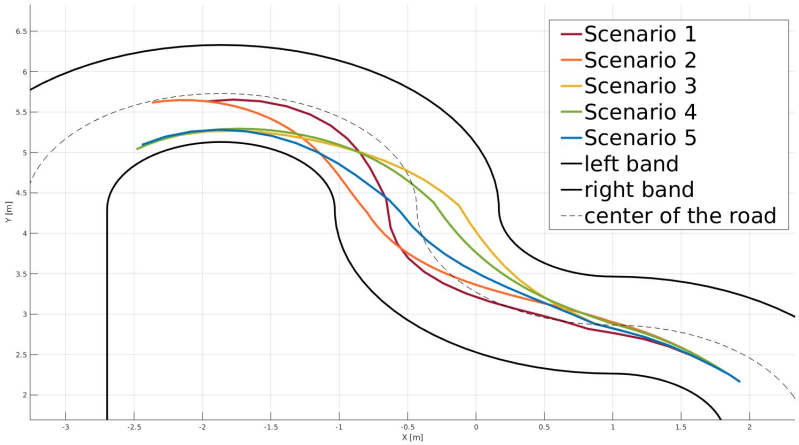

Figure 7.1: Path planned for different H_p and T_s.

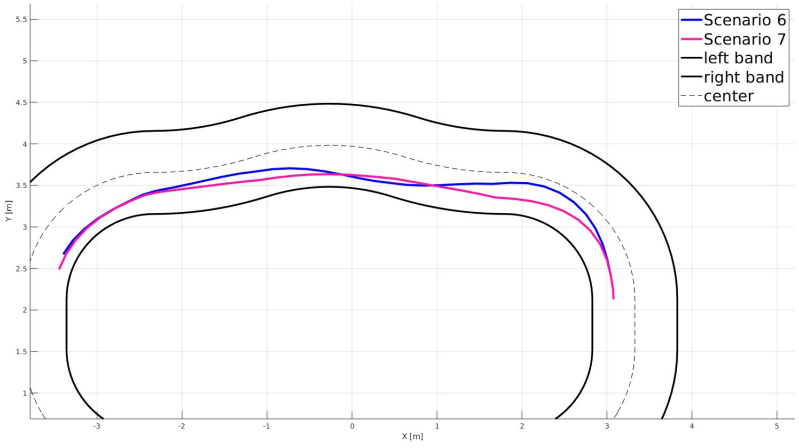

Figure 7.2: Path planned for different H_p and T_s.

From this study it can be concluded what was advanced in Chapter 6, it is relevant to find a trade-off between an admissible computational cost and the length of the path without forgetting that increasing T_s also means increasing discretization uncertainties. Obviously, it can be thought that the ideal case would be to have a sampling time close to zero, and a very large trajectory, but in fact that is not useful because the optimization problem would be solved based on a distant future which will be different to the expected when reached. Therefore, for

the next study it has been selected a big enough T_s that allow the planner designs a large path without needing a very high H_p.

7.1.3 Influence of Weight Tuning on Obstacle Avoidance

At Chapter 5 the obstacle avoidance protocol was described. In this section it is shown the importance of a proper optimization weights selection while the methodology is put in practice. Different simulations have been performed modifying the relevance of weights associated to the performance (Q, L, R and S) with the weight P whose contribution is to reduce the efficiency of the trajectory in order to establish a safety margin between the vehicle and the limits of the road or obstacles. Those simulations are represented at Figure 7.3 and are very useful to understand the relevance of the parameter P.

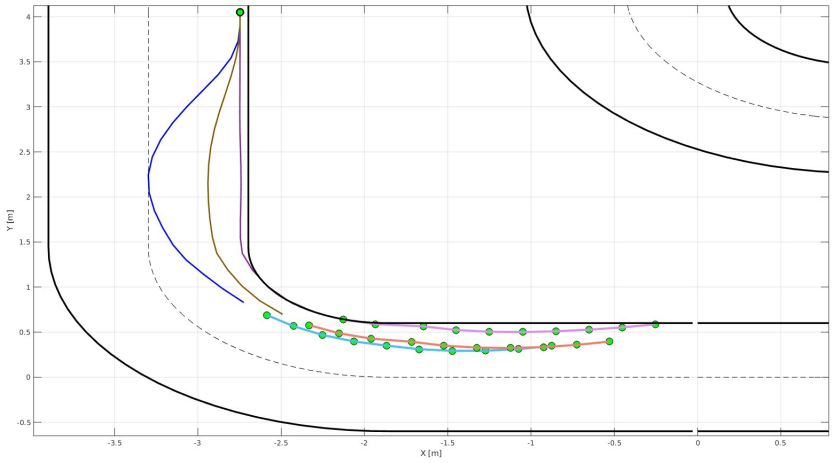

Figure 7.3: Comparison between different safety weights.

The brown dark curve represents the trajectory performed of a vehicle with the same weights as in the previous study (7.6), while the orange curve is the designed path for following steps. The purple curves have been generated reducing 1000 times the magnitude of P keeping the other weights as in (7.6). Finally, the blue curves have been generated increasing 1000 times the magnitude of 1000.
Comparing the three trajectories generated, an insignificant weight P does not keep the vehicle away from the margins prioritizing the efficiency of the trajectory. This result is undesired

because the uncertainty of the model or the estimation may induce the vehicle to a position where a future collision is not avoidable. On the other hand, giving an oversized magnitude to the parameter P will prioritize safety to efficiency, obtaining a poor performance. Therefore, it is important to tune this parameter with a proper magnitude finding an engagement between guaranteeing safety and obtaining efficient results as the ones obtained with configuration (7.6).

7.1.3.1 Validation of Obstacle Avoidance Protocol

Four obstacles have been distributed along the circuit. One is located at the left side of the road, another at the right side and the other two vehicles are driving in parallel. The four vehicles are driving straight forward with a constant increment of their state s, while their distance to the center of the road varies according to a sinusoidal function.
The simulation has been performed using map "L_shape" to study the obstacle avoidance protocol in a scenario with curvature changes.

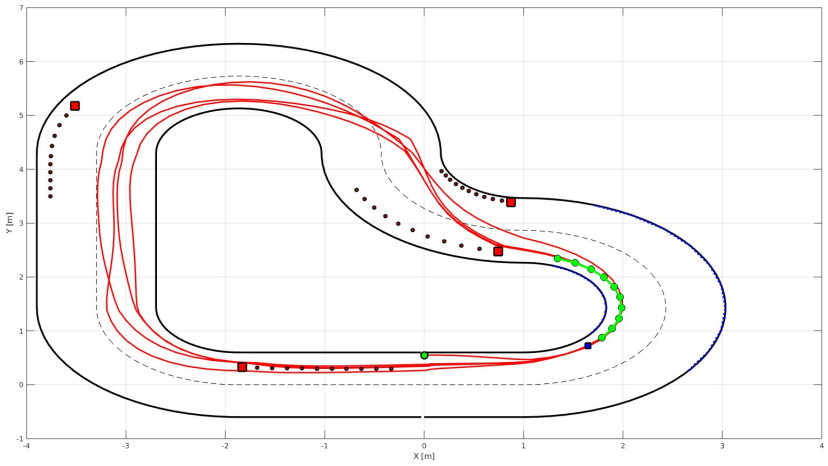

Figure 7.4: Trajectory performed using the kinematic NL-MP.

Figure 7.4 shows the result of performing a simulation of 35 seconds with the weights used for the previous study (7.6).
The red curve represents the trajectory already performed, the green doted one the planned for following steps, the green dot the initial position, the blue square, the current position, and the red squares and dots are the obstacles current and estimated following positions. The blue doted lines are the lateral margins considered for the optimization problem in order to design

a safety trajectory.

As it can be seen, the vehicle has performed different trajectories at each round looking for the most efficient path adapting it to the obstacles to avoid. Thus, in the second round, the last curve (bottom-right corner) the vehicle drives closer to the center of the road because two obstacles were avoided as it can be seen at Figure 7.6. Same happens with the upper curve, in two of the four rounds the vehicle has avoided an obstacle thanks to the coordination protocol. An example of the first round has been plotted at Figure 7.5.

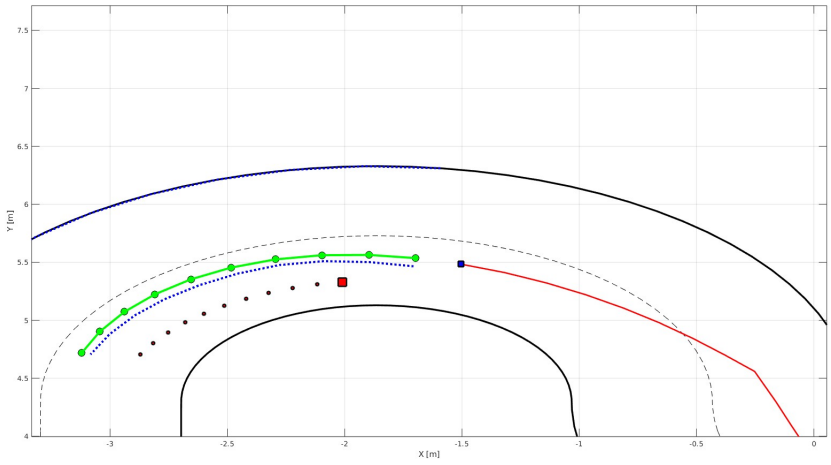

Figure 7.5: Obstacle avoided in a curve of the L_shape map.

7.1.4 Disadvantages and Faced Problems

The use of a kinematic model instead of a dynamic simplifies the model considerably but introduces uncertainties to the system. In addition, the non-linearities of the system induce high computational costs which are not admissible. Both problems have resulted in difficulties when trying to perform more realistic simulations using the ODE system developed (described at Chapter 6). Only simulations with unrealistic low sampling times and very conservative weights were able to be computed. Nevertheless, many simulations where stopped by the solvers arguing feasibility problems or too many time computing an iteration.
To avoid linearizations, an LPV approach was considered but as mentioned in Chapter 3, the resulting LPV state-space representation is not fully controllable, being impossible to design a motion planner which guarantees safety.

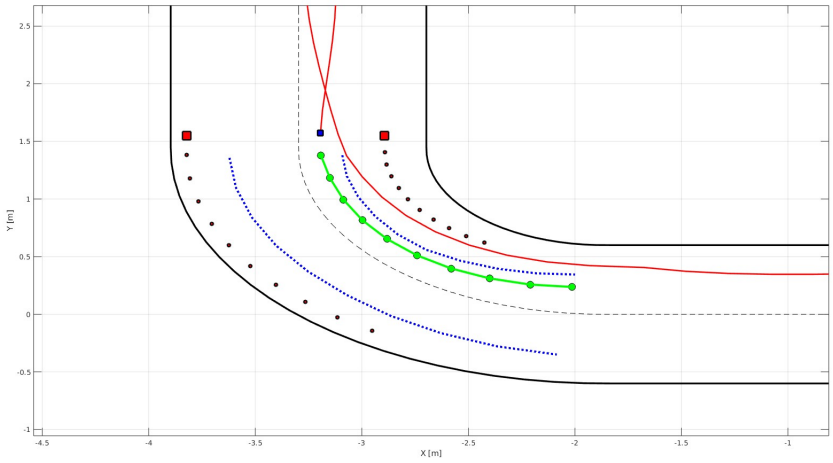

Figure 7.6: Obstacles in parallel avoided on the L_shape map.

Finally, after having proved how powerful this planners could be, it has been decided to explore other ways by changing the model to a dynamic one which can be represented as a fully controllable system. Some approximations and constraints have been necessary to guarantee the controllability as explained at Chapter 4.

7.2 NL Dynamic-Based MP

To solve the controllability issues of the previous planner, this MP makes use of the model described in Chapter 4 with the vehicle parameterized with the same configuration as the NL kinematic-based MP (the parameters detailed at Chapter 6). Once again, the solver used has been "fmincon" because of being working with non-linear constraints.
The structure of the weights proposed is slightly different to the previous planner because of counting with different states and inputs but the idea is, in essence, keep a similar statement of the cost function rewarding high velocities while keeping away from obstacles and the road limits designing an efficient path. Resulting formulation is presented from equation (7.7) to (7.11).

$$Q = \begin{bmatrix} \frac{q_1}{v_{x,max}^2} & 0 & 0 & 0 & 0 & 0 \\ 0 & 0 & 0 & 0 & 0 & 0 \\ 0 & 0 & 0 & 0 & 0 & 0 \\ 0 & 0 & 0 & 0 & 0 & 0 \\ 0 & 0 & 0 & 0 & 0 & 0 \end{bmatrix} \tag{7.7}$$

$$L = \begin{bmatrix} \frac{l_1}{v_{x,max}} & 0 & 0 & 0 & 0 & 0 \end{bmatrix}^T \tag{7.8}$$

$$R = \begin{bmatrix} \frac{r_1}{a_{max}^2} & 0 & 0 & 0 \\ 0 & 0 & 0 & 0 \\ 0 & 0 & 0 & 0 \\ 0 & 0 & 0 & \frac{r_2}{\Delta\delta_{max}} \end{bmatrix} \tag{7.9}$$

$$P = \begin{bmatrix} \frac{p_1}{max-halfwidth^2} \end{bmatrix} \tag{7.10}$$

$$S = \begin{bmatrix} \frac{s_1}{H_p \cdot T_s \cdot v_{x,max}} \end{bmatrix} \tag{7.11}$$

As the planner need to be initialized a vector with the following expected curvatures of the road, the simulations have been performed starting at locations where the curvature is expected to be constant in, at least, some iterations.

7.2.1 Results

To validate the planner, it has been simulated the vehicle with the L_shape map. The values of the weights used are the presented at 7.12. Once again, 4 obstacles have been introduced, one at the right side, another at the left side, and two vehicles driving in parallel at both sides of the road. As initial states, the vehicles has been centered at the initial position of the map with an initial linear speed of 1,5 m/s. In order to simplify the simulations, it has been considered the vehicle has a motion controller implemented with enough accuracy to consider the path tracking perfect.

$$q_1 = -\frac{14}{H_p}; l_1 = -\frac{1}{H_p}; r_1 = \frac{400}{H_p}; r_2 = \frac{6219,112}{H_p}; s_1 = -18000 \tag{7.12}$$

Figure 7.7 shows the trajectory performed after 100 iterations using a sample time of 0,05 seconds and a prediction horizon of 10 samples. Certifying the results are similar to the obtained with the previous MP and can avoid the obstacles thanks to the protocol implemented.

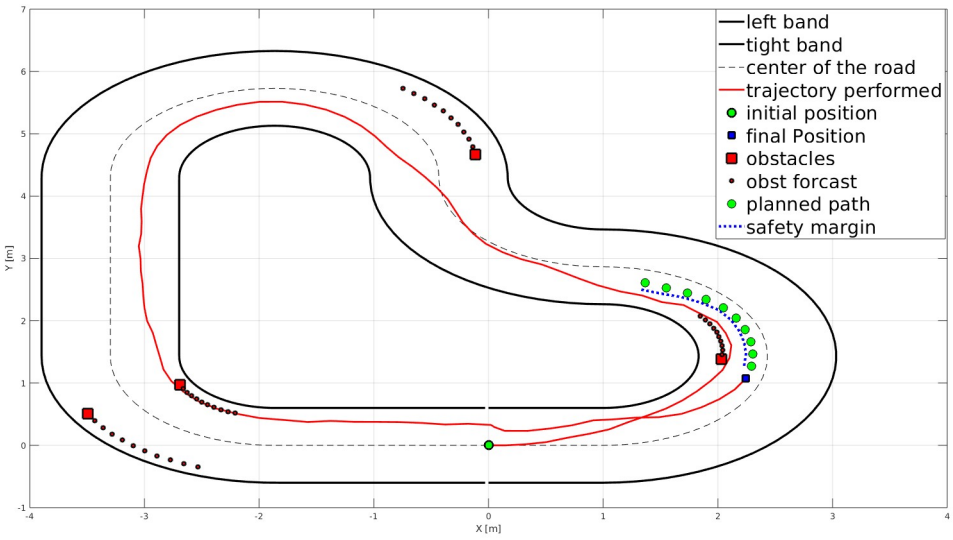

Figure 7.7: NL Dynamic-Based MP at L_shape

In addition, it has been tested under the same conditions as the NL kinematic-based MP, obtaining the following results for the different H_p and T_s used.
The Table of Results 7.2 proofs that increasing the complexity of the model also means increasing computational costs to really high values. More scenarios were tried to be simulated, but the solvers were not able to provide a solution arguing too much time needed to compute each iteration. The three that have been successfully computed have been plotted at Figure 7.8, where once again it is observed the relevance of choosing a high H_p to obtain a smoother path.

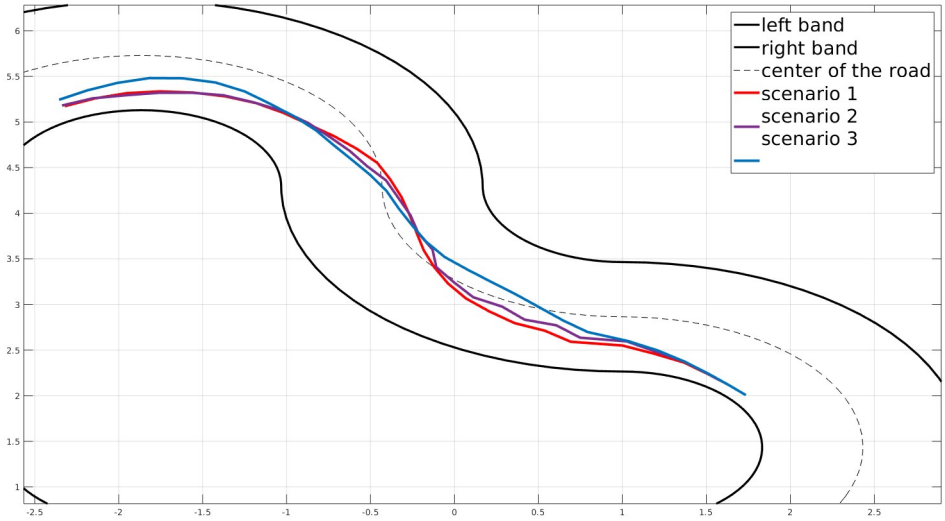

Figure 7.8: NL Dynamic-Based MP at L_shape

7.2.2 Disadvantages and Faced Problems

The aim of designing this motion planner was just to verify its functionality and use it as a step between the non-linear MP based on the kinematic model, and the LPV MP based on the dynamic bicycle model.

As expected, the computational cost was even if higher than the undesired results from the other MP. Even more problematic has been the resolution of the optimization problem. The increment of complexity has been translated in more complex cost functions which are not supported by the solvers available.

With all this information, it is clear the need of applying LPV techniques to reduce computational costs although it could imply a reduction in the quality of the solution.

	H_p	T_s [s]	$H_p \cdot T_s$ [s]	$T_{compu}[s]$	$\Delta s[m]$
Scenario 1	5	0,1	0,5	0,336316	6,487733
Scenario 2	7	0,1	0,7	0,677322	6,503277
Scenario 3	10	0,1	1	1,389133	6,484308

Table 7.2: Results of simulations with different H_p-T_s.

Chapter 8

LPV Motion Planner

The aim of this chapter is to describe the procedure and results obtained of having designed a new MP based on the dynamic bicycle model and studied as a quadratic optimization problem using LPV techniques.

8.1 Inclusion of LPVs

The first aspect to consider in comparison with the previous MP is how to deal with the LPV matrices and what can be expected from them.

The idea of this MP is to have a linear-quadratic optimization problem with linear constraints, reducing significantly the computational cost of the problem. Therefore, the non-linearities are embedded in a previous stage to the optimization problem which has been called "LPV generation".
At this stage of motion planning, it is analyzed the current state of the vehicle and the previous planned sequence of states and inputs for the following H_p time instants. With this information and solving non-linear calculations, the evolution of the system gets approximated by a sequence of matrices associated to each time instant and states-inputs planned. Those linear expressions are the ones used for the optimization problem, reducing the computational complexity while the uncertainty of the results increases. A graphical representation of how it works can be consulted at Figure 8.1.
It is important to remark this aspect because the more distanced the samples along time, less accurate is the model used for designing the path.
Additionally, larger temporal paths ($H_p \cdot T_s$) include more cumulative error being the result less trustworthy. In fact, choosing big T_s or high values of H_p may stack the solvers by infeasible

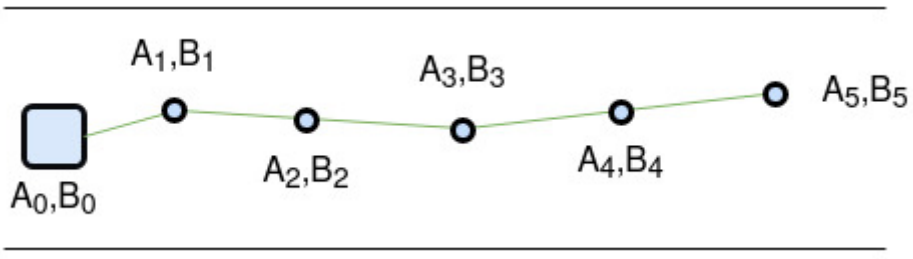

Figure 8.1: States used for the LPV matrices based on the previous path designed.

problems or exceeding the maximal computation time per iteration allowed. Therefore, a good criterion for choosing both parameters could be based not on increasing the total temporal length of the path but finding a configuration which allows solving the optimization problem fast enough while including many samples along the path in order to be accurate without compromising the safety of the vehicle and liveness of the passengers.

8.1.1 Initialization of the MP

As the first iteration makes use not only of a vector with curvatures expected but also of a set of A and B LPV matrices, the expected state values have been obtained by performing a simulation with the ODE45 model of the vehicle supposing maximal acceleration and no variation of the steering angle. Also, the curvature at those points is consulted from the map in order to execute the planner with the most accurate information as possible.
For this family of MP the "fmincon" solver is not useful anymore and has been replaced by the "Quadprog" solver, which is a specific solver for quadratic-linear optimization functions with linear constraints.

8.2 LPV Motion Planner

Because of using the same model as the dynamic-based NL-MP, the influence and the structure of the weights is the same, but new terms have been added to improve the performance. Thus, the structure of the matrix is the defined from (8.1) to (8.5).

As novelty compared with the NL-MP already studied, the simulations performed at this chapter make use of the ODE45 model as ground truth. That is, once the path is designed, the

state value for the next iteration is obtained from applying the first input of the sequence to the non-linear dynamic model expressed by differential equations.

$$Q = \begin{bmatrix} \frac{q_1}{v_{x,max}^2} & 0 & 0 & 0 & 0 & 0 \\ 0 & 0 & 0 & 0 & 0 & 0 \\ 0 & 0 & 0 & 0 & 0 & 0 \\ 0 & 0 & 0 & 0 & 0 & 0 \\ 0 & 0 & 0 & 0 & 0 & 0 \\ 0 & 0 & 0 & 0 & 0 & 0 \end{bmatrix} \tag{8.1}$$

$$L = \begin{bmatrix} \frac{l_1}{v_{x,max}} & 0 & 0 & 0 & 0 & 0 \end{bmatrix}^T \tag{8.2}$$

$$R = \begin{bmatrix} \frac{r_1}{a_{max}^2} & 0 & 0 & 0 \\ 0 & \frac{r_2}{\delta_{max}^2} & 0 & 0 \\ 0 & 0 & \frac{r_3}{\Delta a_{max}^2} & 0 \\ 0 & 0 & 0 & \frac{r_4}{\Delta \delta_{max}} \end{bmatrix} \tag{8.3}$$

$$P = \begin{bmatrix} \frac{p_1}{max - halfwidth^2} \end{bmatrix} \tag{8.4}$$

$$S = \begin{bmatrix} \frac{s_1}{H_p \cdot T_s \cdot v_{max}} \end{bmatrix} \tag{8.5}$$

A good manner of seeing that the inclusion of LPV matrices and changing the solver implies a difference in the result is by simulating the MP with same configuration. For this aim, a first simulation has been performed with the parameters used previously which are the detailed at (8.6).

$$q_1 = -\frac{14}{H_p}; l_1 = -\frac{1}{H_p}; r_1 = \frac{400}{H_p}; r_2 = \frac{0}{H_p}; r_3 = \frac{0}{H_p}; r_4 = \frac{6219,112}{H_p}; s_1 = -18000 \tag{8.6}$$

As it can be observed at the Table of Results 8.1, the temporal length of each path designed

	H_p	T_s [s]	$H_p \cdot T_s$ [s]	$T_{compu}[s]$	$\Delta s[m]$
Scenario 1	30	0,015	0,45	0,0872210	11,100554
Scenario 2	30	0,02	0,6	0,0865656	11,532710
Scenario 3	10	0,03	0,3	0,0294499	11,128865
Scenario 4	40	0,01	0,4	0,128792	11,100461
Scenario 5	10	0,06	0,6	0,0257505	11,563888

Table 8.1: Results of simulations with different H_p-T_s.

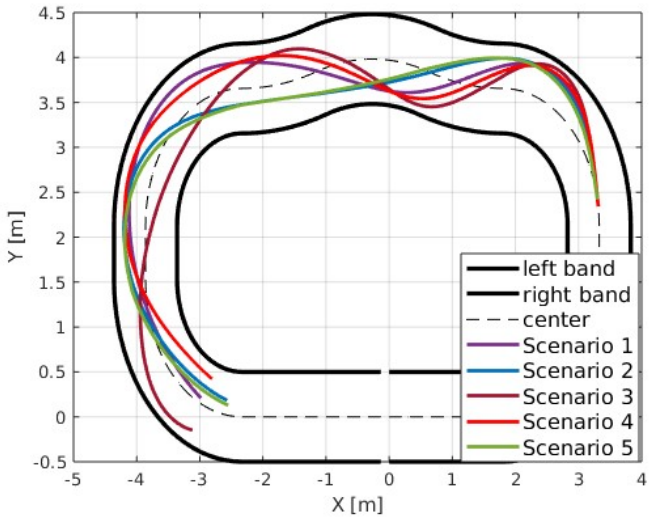

Figure 8.2: LPV-MP with different H_p-T_s at map 3110.

is generally shorter as in previous planers because of computational issues. When it was tried to use a bigger sampling time or higher prediction horizon, feasibility issues associated to the solvers appeared.

What is also noticeable is the computational cost of each iteration. Comparing it with previous planners, although having introduced a new step to compute the matrices, the duration of each iteration is significantly lower, but the solver still takes more time at each iteration than the T_s associated. However, this problematic is expected to be solved in case of using more efficient solvers.

8.2.1 Tuning of New Weights

Taking this into account the paths planned in the five scenarios, other weights can be considered. In fact, it is also interesting to observe the states followed and the input suggested. For example, Figures 8.4 and 8.3 show the path followed using a prediction horizon of 40 samples and a sampling time of 0,025 seconds and the value of the states and input proposed at each iteration avoiding obstacles in map "L_shape". The simulation represents the car driving during 11,25 seconds.

Having used a path with a temporal length of 1 second and many samples during it, the

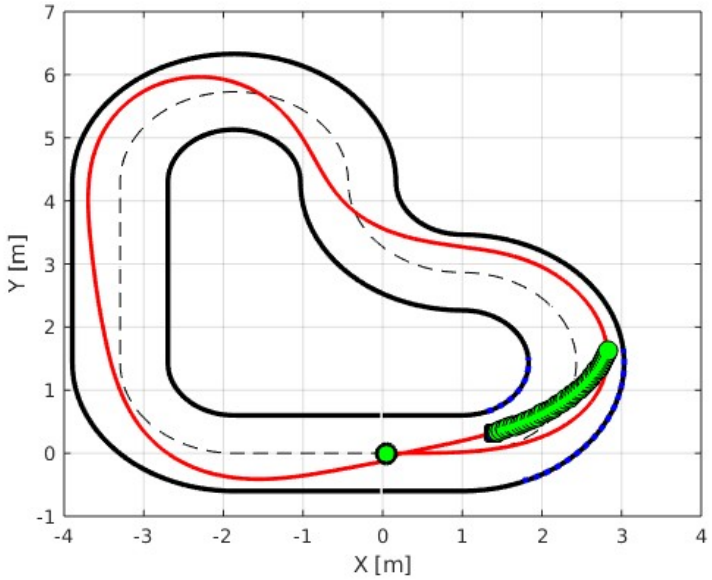

Figure 8.3: Trajectory followed with the weights chosen for the NL-MP.

way the vehicle drives along the curves is very smooth and does not correspond at all with the behaviour of the previous solvers. For this reason, the weights have been changed to obtain a more efficient planner improving the distance traveled in the same period of time.
After trying different configurations, the tuning found which offer a good trade-off between an efficient and a comfortable performance is using the same matrices but parameterized with the weights with the values presented at (8.7). A simulation of 8,75 seconds over the same map and same initial conditions have been performed. Results are shown at Figures 8.5 and 8.6.

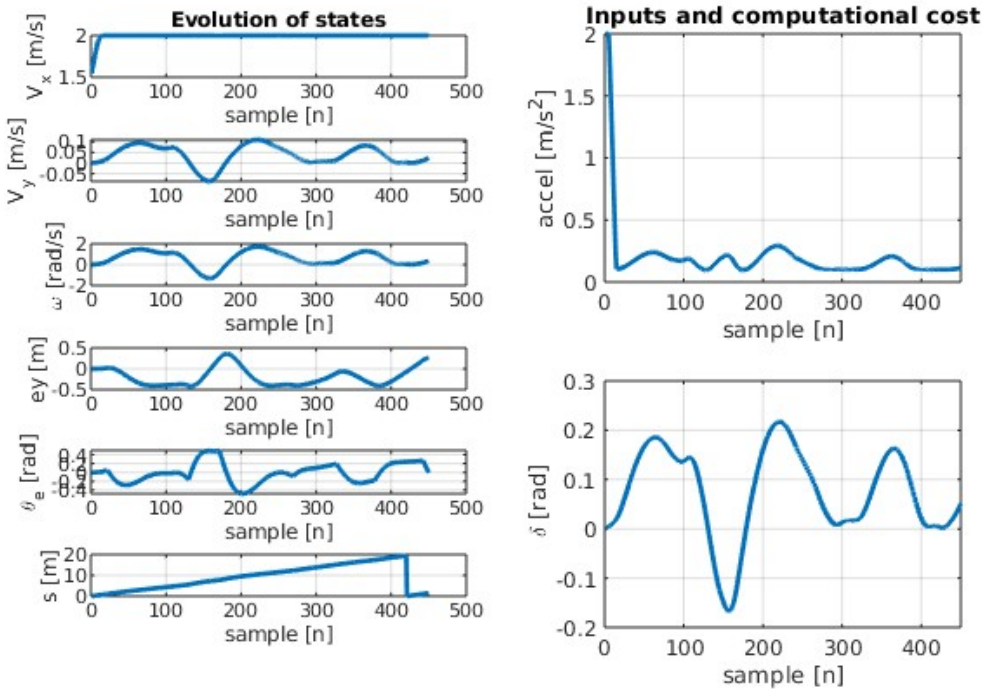

Figure 8.4: Inputs and states over the trajectory represented at Figure 8.3.

$$q_1 = -\frac{14}{H_p}; l_1 = -\frac{1}{H_p}; r_1 = \frac{1,3}{H_p}; r_2 = \frac{4000}{H_p}; r_3 = \frac{40}{H_p}; r_4 = \frac{20,73}{H_p}; s_1 = -18000 \tag{8.7}$$

In case of including obstacles, the results are quite similar but reducing the distance. At Figure 8.7 can be consulted a frame of a simulation including obstacles.

At this point it, the next stage to explain of the MP designed is the inclusion of viability analysis to guarantee safety. Because of its high theoretical content and its relevance over the project, this MP is explained in an independent chapter.

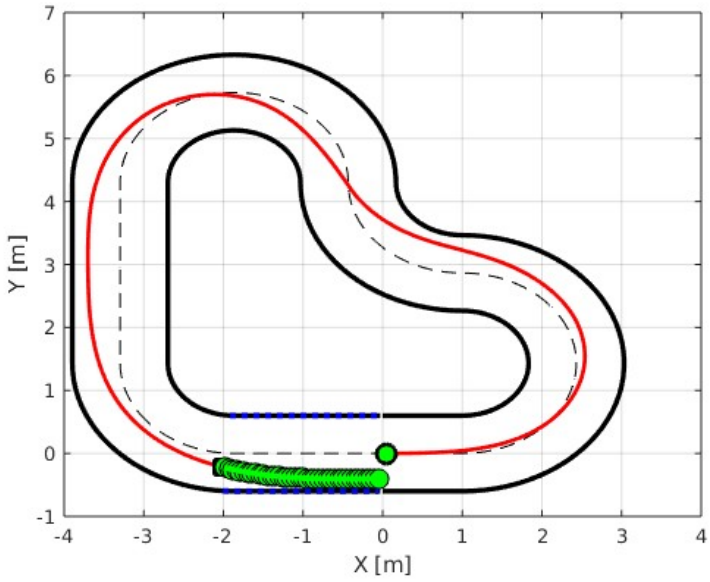

Figure 8.5: Trajectory followed with the new weights chosen.

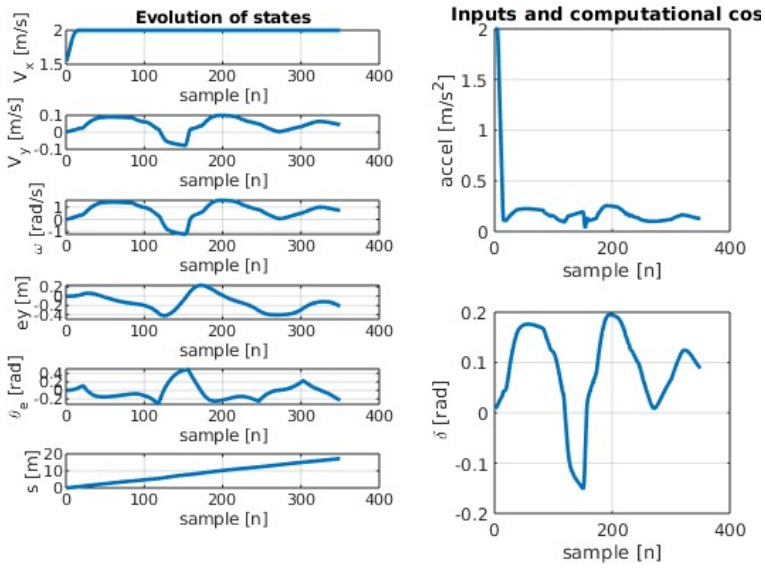

Figure 8.6: Inputs and states over the trajectory represented at Figure 8.5.

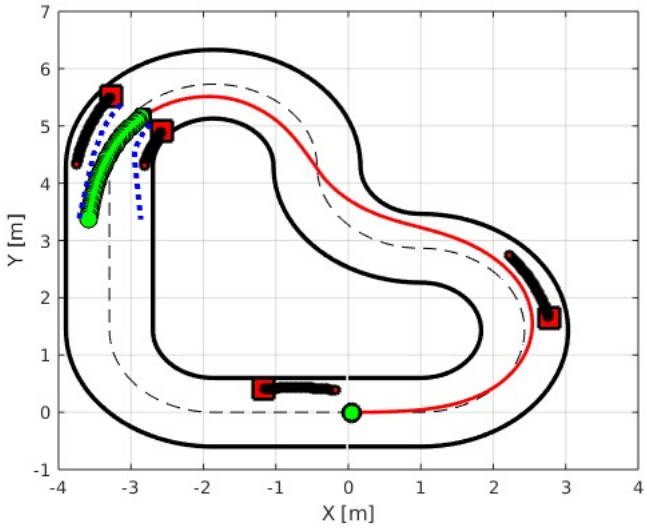

Figure 8.7: Trajectory followed avoiding obstacles with the new weights.

Chapter 9

Zonotope-tube-based LPV Motion Planner

The aim of this chapter is to describe the procedure and results obtained of introducing an algorithm focused on guaranteeing safety based on propagating set of states along time to constraint the problem.

9.1 Theoretical Approach

The inclusion of set propagation can be seen as a safety mechanism focused on increasing the robustness of the solution. It is stated as a previous stage to the planner to define the constraints of the optimization problem once the LPV matrices and the propagation of obstacles are already computed.
The idea is to propose a change of paradigm by considering states as sets. That is, instead of estimating a state as the most probable value, or as a distribution with the center and the uncertainty, now the idea is to compute a set of states (or inputs) which guarantees the real state is inside. Thus, if the set definition is faithful to reality and accomplishes the specifications, performance and safety conditions are guaranteed independently by the real states if it is located inside the set.

9.1.1 Zonotopes

This powerful tool has an untapped potential which faces computational issues. Generally, research works have been using ellipsoidal sets to represent the set of states, but recently a new

type of set called zonotopes has been introduced.
As explained at [21], a zonotope can be defined as the center of the set (p_x), and the generator matrix (H_x) which defines the shape of the zonotope being L^r a vector of independent parameters λ_i which can take any value inside the interval [-1,1]. The resulting formulation would be as at (9.2).

$$S_i = p_x \oplus H_x L^r \tag{9.1}$$

$$A \cdot S_i = A \cdot p_i \oplus B \cdot H_i L^r \tag{9.2}$$

Then:

$$S_x^{k+1} = A \cdot S_x^k + B \cdot S_u^k \tag{9.3}$$

$$p_x^{k+1} = A \cdot p_x^k + B \cdot p_u^k \tag{9.4}$$

$$H_x k^{k+1} = [A \cdot H_x^k | B \cdot H_u^k] \tag{9.5}$$

As reference, it has been used the scientific paper [22]. Although it is focused on another topic, there is described how easy is the propagation of a zonotope using the Minkowski sum and the idea of computing inverse images of a propagated set to obtain the subset of valid inputs. Those concepts are explained and used in following sections.
The main disadvantage of the zonotopes is the methodology of computing intersections, being approximations whose computational cost or final results are not always desirable. The other disadvantage is the increment of complexity when increasing the number of propagation steps, obtaining a big matrix L^r where many of its component do not make a big contribution to the shape of the zonotope.
Therefore, sometimes intervals have been used to simplify the computation while compromising the quality of the solution.
To facilitate the implementation, a free toolbox called CORA has been used that many tools to define and operate with sets are already implemented.

9.2 Implementation Using Zonotopes

The following list shows the steps followed at each iteration of the algorithm developed, which is described immediately bellow.

- Computation of the set of inputs which could be applied based on the previous inputs

and the maximal increment allowed.

- Constraint the possible inputs according to their upper and lower bounds.
- Propagation of the set of states with the LPV matrices and the set of inputs computed.
- Constraint the possible states according to their upper and lower bounds.
- Computation of the subset of inputs which can produce those states based on an inverse propagation (Over-approach).
- Certify the fulfillment of constraints
- Cover the zonotopes with a box which is used as intervals of constraints for the optimization problem.

First of all, it is computed the set of inputs which can be applied. For that, the last set of inputs applied (or suggested) is modeled as a zonotope and increased according to the allowed increments of the inputs (limits of the slew rates). Once the new set is defined, it is constrained according to the upper and lower bound of the inputs. It has been graphically explained at Figure 9.1 and mathematically formulated at (9.6).

$$\hat{S}_u^k = \left(S_u^{k-1} + S_{\Delta u}\right) \cap S_u^C \tag{9.6}$$

Once a first input $\hat{S}_u$ has been computed, the next step followed is the propagation of the

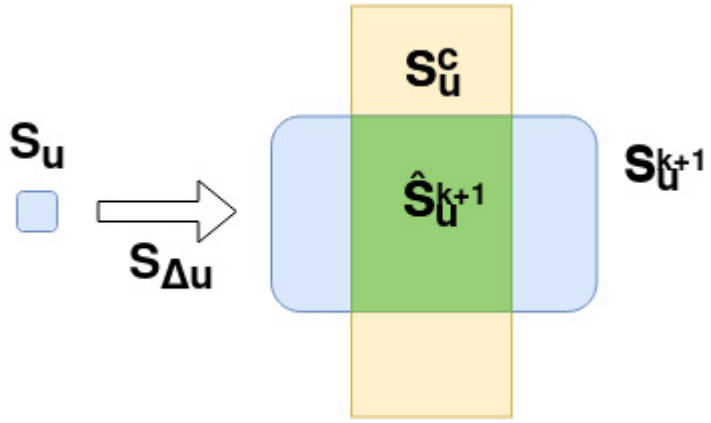

Figure 9.1: Propagation of the input

set of states as described at (9.5). For this step, the matrices A and B are needed. Until now, the matrices used are those LPV matrices computed with the desired states at each time instant based on the last path designed. In a future it would be interesting to analyze other alternatives such as computing the matrices for the center of the last zonotope of the tube (and execute iteratively enlarging the tube), or using matrices which takes into account the uncertainty. That means, a set of matrices considering the exact evolution of all states inside the set. Another relevant aspect to remark is the exclusion of the sixth state. As it has been mentioned several times along this document, the dynamic model counts with a state s which is useful for evaluating the trajectory planned but is unconstrained and does not influence in the dynamic of the other five states. Therefore, it has been excluded from the propagation of states, reducing the problem to the five main magnitudes: $[v_x, v_y, \omega, e_y, \theta_e]$.

It is analyzed if the propagated zonotope is contained inside the constraints of the system to validate all the possible states and inputs studied. Otherwise, it is computed the intersection between states which are reachable and constraints with two aims: On one side, it is constrained to delete those states with are not compatible with the environmental and physical constraints of the problem. On the other side, the inverse image of the constrained set is computed to delete those inputs which do not generate a valid solution. For this calculus is used the pseudo-inverse matrix of B and the original set of states.
In other words, a reachability analysis is performed, and those states and inputs which do not produce a valid solution are deleted from the original sets.
The computation of the resulting constrained states-set and the resulting constrained inputs-set are graphically represented at Figure 9.2 and mathematically defined at (9.7) and (9.8) respectively.

$$\hat{S}_x^{k+1} = \left(AS_u^k + B\hat{S}_u^k\right) \cap S_x^{C_k} \tag{9.7}$$

$$S_u^k = B^+ \left(S_x^{k+1} \sim AS_x^k\right) \quad S_u^k \subseteq \hat{S}_u^k \tag{9.8}$$

As it has been already commented, there is an inconvenience of using CORA. The intersection between two zonotopes does not result on another zonotope, and the toolbox applies an

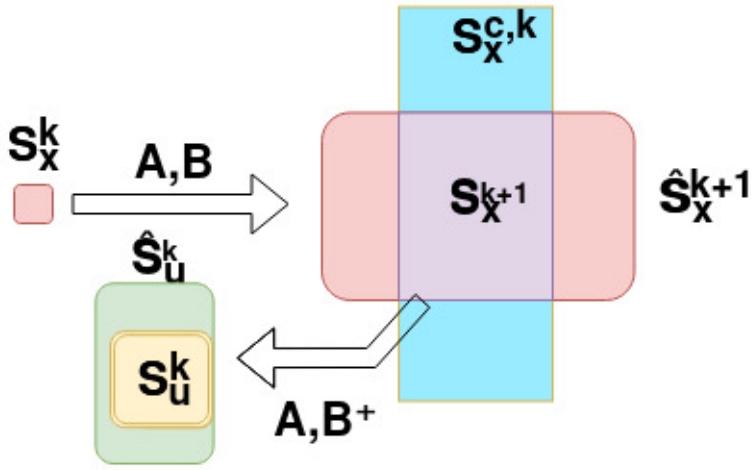

Figure 9.2: Computation of the constrained states and inputs.

over-approximation computing the smallest zonotope of a certain number of generators which contains the intersection. To simplify the cost, the distance between two zonotopes at (9.8) and the intersection between the inverse image and the original set of inputs $\hat{S}_u^k$ have been studied as intervals instead of zonotopes.

Finally, it has been computed the smallest boxes which contain the final sets to use them as constraints of the planner explained in previous Chapter 8.
As it can be observed at Figure 9.3, depending on the shape of the zonotope, some invalid or impossible solutions may be included in the optimization problem, but the region to study will be significantly lower than in previous planners reducing the problem. This aspect should be studied in more detail trying to find more precisely solutions, such as expressing the constraint of the problem as zonotopes, but without forgetting the relevance of the computational cost.

9.3 Results

Different simulations have been performed to prove its ability avoiding obstacles.

Firstly, it has been used the map "3110" starting centered at the beginning with an initial velocity of 1,5 m/s and an acceleration of 2 m/s^2. The weights used are the same as the specifically designed for the LPV-MP. A prediction horizon of 30 samples with a sampling time of 0,035 seconds has been selected. The simulation has been performed during 12,25 seconds displaying the obstacles as in the other simulations.

Results of the states evolution and the inputs applied can be consulted at Figure 9.4. The trajectory that the ODE45 has travelled has been represented at Figure 9.5. As in previous simulations, the red line represents the trajectory travelled, the red squares the obstacles, the red dots, the estimation of future states of the obstacles, the blue lines, the safety margins considered, the green circle the initial position and the blue square the final position. Green line is the last result of the MP, being the dots the specific locations at each sampling time.

A second simulation has been performed over the "L_shape" map, which is the more complex of all of them due to its curvature. The length of the simulation, the weights and the parameters H_p and T_s have been kept as before. The results have been satisfactory and can be consulted at Figures 9.6 and 9.7.

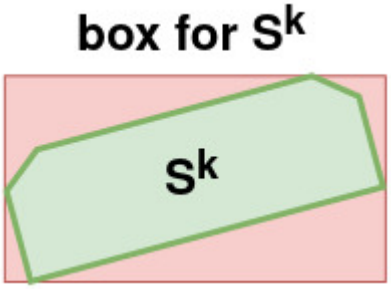

Figure 9.3: Box generated for a zonotopic set.

9.4 Comparison with the LPV-MP

Once it has been proved the zonotopic-tube-based LPV-MP works in different scenarios, a comparison of two planners have been performed. On one hand, planner 1 is the one described at this section. On the other hand, planner 2 is exactly the same but excluding the computation of the tube. By this way it can be studied the impact of introducing it on the computational time of each iteration.
The simulations have been performed at map "L_shape" with an initial linear velocity of 1,5 m/s, a lateral displacement of 0,2 meters and staring at 4 meters from the beginning, to be located just before the curves. The simulation has been performed during 3 seconds using a sampling time of 0,03 seconds. No obstacles were introduced.

The results are shown at Table 9.1 where the third and forth column make reference to the results of the tube-base MP, while the last two ones to the previous studied MP. Same results have been plotted in two graphics at Figure 9.8.

The results of the zonotope-tube-based LPV MP validate the performance of this MP while some aspects of the comparison should be commented.

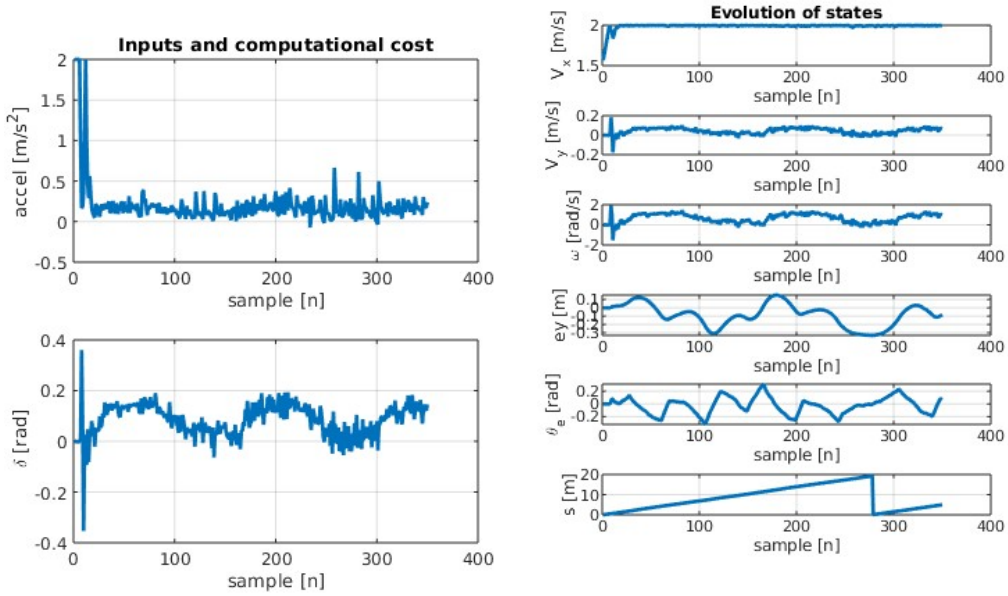

Figure 9.4: Scenario A: Results of the MP at map "3110".

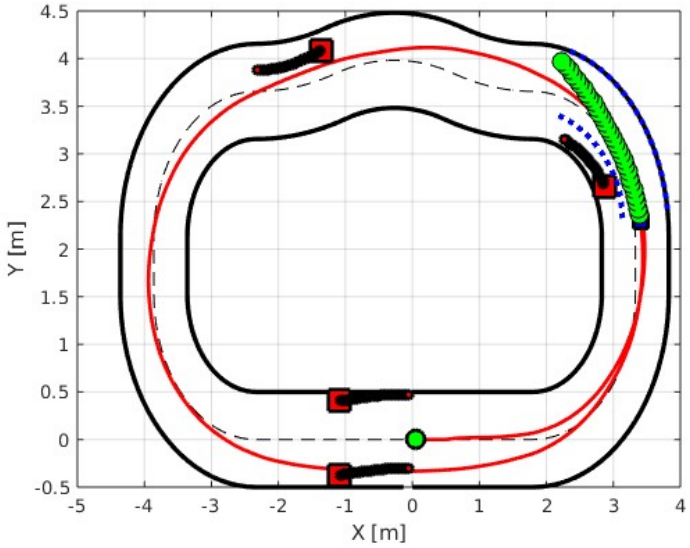

Figure 9.5: Scenario A: Trajectory followed at map "3110".

As expected, planing with a longer prediction horizon improves the result of the trajectory followed while increase the computational cost. Additionally, it can be observed at the first graph of Figure 9.8 that the increment of computational cost is bigger when the safety stage is

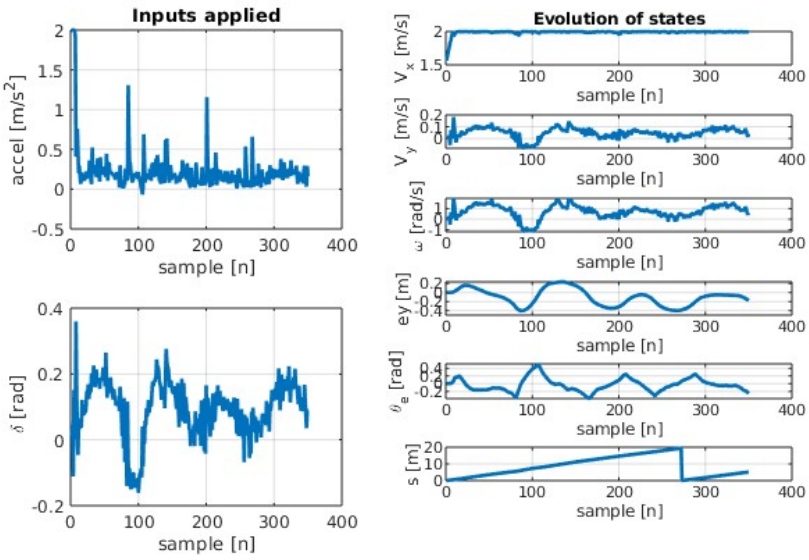

Figure 9.6: Scenario B: Results of the MP at map "L_shape".

	H_p	$H_p \cdot T_s$ [s]	$T_{compu}1[s]$	$\Delta s1[m]$	$T_{compu}2[s]$	$\Delta s2[m]$
Scenario 1	10	0,3	0,0399270	5,987878	0,0846807	6,335604
Scenario 2	20	0,6	0,0739156	6,230370	0,0450907	6,172679
Scenario 3	30	0,9	0,139963	6,315016	0,0846807	6,335604
Scenario 4	40	1,2	0,195420	6,528255	0,128273	6,482221
Scenario 5	50	1,15	0,266810	6,734289	0,163969	6,652345

Table 9.1: Comparison between LPV-MP with (1) and without (2) zonotopic propagation.

included.

To conclude, it is important to remark that, once again, the computational cost is higher than desired because it is not assumable that each path takes more time to be designed that the sampling time. Other alternatives like more efficient solvers or considering the use of different magnitudes for sampling and discretization time should be studied.

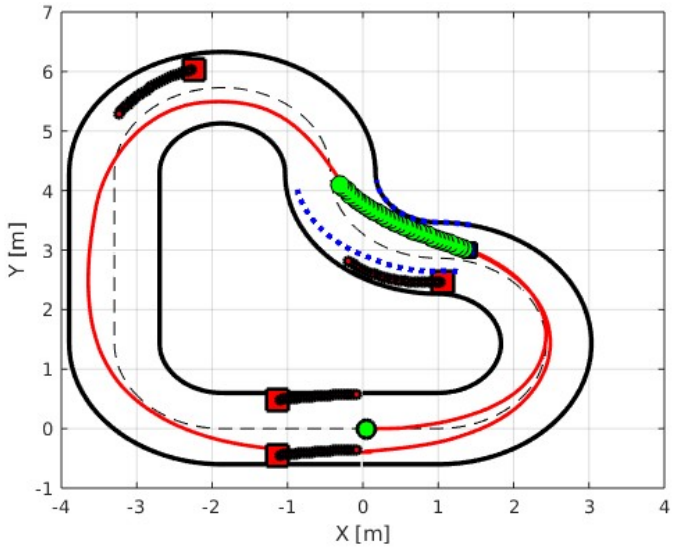

Figure 9.7: Scenario B: Trajectory followed at map "L_shape".

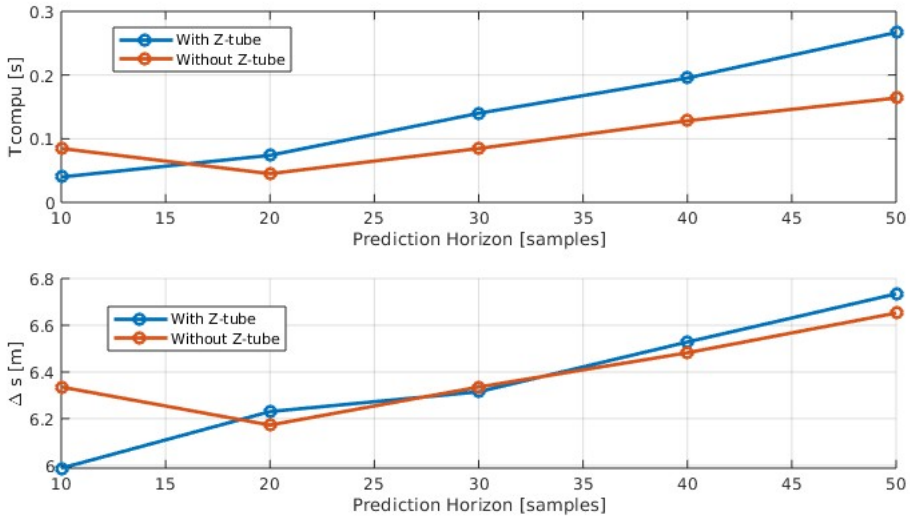

Figure 9.8: Comparison between LPV-MP with and without zonotopic propagation.

Chapter 10

Conclusions and Future Work

This TFM presented a study of coordination of autonomous vehicles considering safety mechanisms.
Along this document different aspects and future challenges of mobility have been presented, focusing on the coordination problematic of V2V (or V2X) communicated vehicles with level of autonomy 5. After analyzing the different approaches proposed by different researchers, it has been considered the possibility of solving part of the problematic designing an optimization-based motion planner (MP) which also includes an obstacles avoidance protocol in the algorithm. In comparison with other publications analyzed, this project proposes a motion planner which is also valid for mobile obstacles (not only statics), studying them from the point of view of set-theory, without forgetting the computational cost problematic by including LPV techniques.

10.1 Conclusions

Along the document different vehicle models have been described and different MP have been developed and studied. After facing controllability problems, it can be said that the kinematic bicycle model use not useful outside non-convex optimization problems and has to be replaced by the dynamic bicycle model although its complexity increases significantly the computational cost.
With regard to computational cost, it has been proved that non-linear problems are not compatible with the performance desired using nowadays technologies, but the results looks promising and could be useful in a future with more powerful computation systems. As presented in the last two previous chapters, the substitution of the non-linear equations by a state-space

representation including LPV matrices reach an important reduction of the computational time without deteriorating the results, making it a suitable alternative.
Finally, a preliminary study of the possibility of including set theory inside the MP to guarantee safety has been certified as something feasible and interesting. Consequently, it remains open a very interesting field to study more in-depth from which we can expect promising results.

10.2 Future work

During the development of the project, many adversities have been faced. Some of them have been solved finding alternatives while others have been left as admissible, like the computational cost, but new alternatives have to be studied. Additionally, a new field of study has been introduced related with the combination of theory set, motion planners and coordination. Many aspects have to be studied to validate the preliminary results obtained as well as many elements could be in-depth studied to improve the performance thanks to its untapped potential. Finally, it would be interesting to perform practical studies implementing it in a vehicle model and validating the result in a real scenario.
The following list present some proposed tasks which can be used as starting point to continue this project:

- Analyze different studies and criteria and adapt the weights of the solvers to a more general concept of what a good performance means.
- Develop a more realistic simulation scenario using a more complete vehicle model for the ground truth and introducing disturbances in the measures. Also other scenarios of obstacles could be considered.
- Repeat the simulations comparing the different MP using more powerful solvers and study the computational costs and feasibility problems simulating the different MP under same conditions.
- Translation of the code to Python or C using ROS libraries and testing the motion planners with a real model.
- Continue the Zonotope-tube-based LPV MP. Many gaps are open being some of them the following ones:
  - Improve the outer-approach of the intersection.

- Use the zonotopes to define the constraints with a more efficient methodology than translating it to intervals.
- Selection of a more realistic state for the design of the LPV matrices.
- Use of a set of matrices for the propagation of the tube.
- Propagate the obstacles with tubes to consider the uncertainty and study collisions as intersection or distance between sets.
- Study the possibility of introducing other type of sets.

Appendix A

Time Planning

As every *R&D* project, a temporary planning is required. In this chapter is presented the one proposed for this work which has been followed throughout its development is presented.

To do present the time planning, it is necessary to start by highlighting that this project has been developed as an extended TFM with a load of 30 ECTS. Being the ECTS a European standard to measure the hours of work of a student, it was expected that this work would be equivalent to approximately 900 hours if each ECTS is evaluated as 30 hours [25].
Expecting a weekly dedication of 37.5 hours equivalents to that of a spanish public worker [27], the planning of the project is distributed in 24 weeks as shown at the following Gantt chart of Figure A.1.

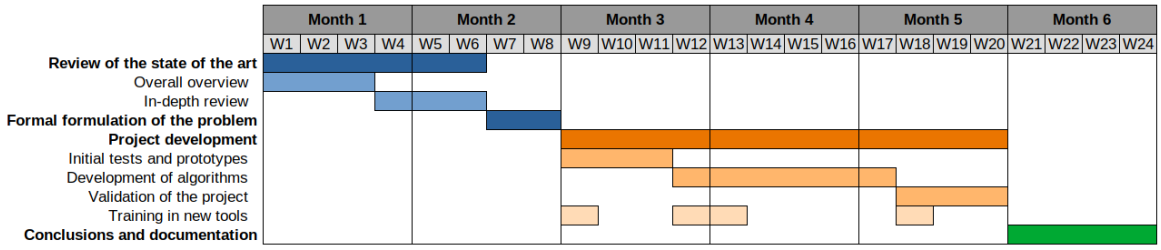

Figure A.1: Gantt chart: showing the temporary distribution of tasks planned.

A.1 Description of the Tasks

The tasks present at the Gantt chart are detailed bellow:

- **Review of the state of the art**: First of all, six weeks were planned to acquire knowledge about the topic and the actual state of the art.
  This task has been divided in two sub-tasks: Firstly, read surveys and generalist papers to understand the actual situation of the technology. Secondly, read more specific papers focused on more detailed issues and specific cases of study.
  Obviously, during the following months more bibliography has been consulted occasionally, but not as main task.

- **Formal formulation of the problem**: Once it was studied the current situation of technologies and algorithms used for coordinating vehicles, it was time to evaluate and design the specific scenario and problematic which to study in order to improve the actual available technologies.
  As it has been explained in previous chapters, this project put the spotlight on improving the coordination of vehicles from the point of view of designing safety and comfortable trajectories.

- **Project development**: Once defined the case of study and how the research is going to be developed, it took place the main part of the project which was expected to take around 12 weeks. Firstly, initial proves and scenarios have been developed. This stage let you realize of new difficulties and hardships which have to be handled. After that, the problem has been slightly reformulated including the new adversities detected and took place the main development of algorithms and proves.Finally, all the algorithms developed were evaluated and compared using different scenarios.
  As it can be seen, an extra sub-task called "Training in new tools" was included in the initial plan because in parallel to the development, it was expected to need time to learn how to use new toolboxes or coding languages such as YALMIP or CORA.

- **Conclusions and documentation**: The final stage of the development of this project has consisted in to collect the results obtained during the development stage, analyze the results obtained, extract conclusions and report all this information at this document.

Appendix B

Economical Budget

The development of this project has required an economical investment which can be estimated analyzing all human and material direct costs associated to the development of it.
When talking about human resources, the tasks chart described at Chapter A planned 900 hours of a junior engineer whose wage has been estimated to 15 €per hour taken into account, not only its wage but also the taxes associated. This implies a total amount of 13500€.
On the other side, the licenses of CORA and YALMIP are free, while the annual license of MATLAB for academic use is 250€, while the Optimization Toolbox used has an annual cost of 100€. Therefore, the costs associated to software applicable to the 6 months can be estimated to 175€.
Also, the cost of the laptop (1500€) has to be included.According to the Spanish Law [14],it is possible to apply a maximal amortization of electronic devices of the 20% in a maximal time horizon of 10 years. Therefore, considering an expecting useful life of 5 years, the cost taken into account for the six months has been 150 €. All costs have been summarized at Table B.1.

Concept charged over the 6 months	**Cost in €**
Matlab: Academic license	125
Matlab: Optimization Toolbox license	50
CORA license	-
MPT3 license	-
YALMIP license	-
Engineer wage	13500
Laptop amortization	150
Budget €	13285

Table B.1: Economical budget for the development of the project

Appendix C

Environmental Impact

As it has been observed throughout this document, this TFM presents a study on the application of specific techniques to a very specific objective in a wide field which is coordination of vehicles, therefore its direct environmental impact is not easily calculable.

C.1 Environmental Impact of Autonomous Vehicles

Nevertheless, from a generalist point of view, the positive impact over the environment is considerable as mentioned at the introduction 1.
An improvement in vehicles coordination does not only mean less time over the road, but also less fuel consumption and a reduction of traffic jams with the acoustic and environmental pollution associated.
Furthermore, a more efficient use of vehicles also implies a larger service life of them, reducing the environmental impact related with the manufacturing process.
Hence, it can be said that this research project is oriented to contribute in the research field of achieving a sustainable mobility from the side of improving vehicles coordination.

C.2 Environmental Footprint of this Project

An estimation of the CO_2 directly emitted during the development of this project is very complicated to compute due to the large number of elements consuming energy and the difficulty to measure the real use of them associated to this project. Therefore, it has been considered that any device which would have been connected independently of whether this project were developed or not such as lights, the monitor used or the internet connection, are not included

in this calculus, taking only into account the direct ecological footprint of the computer used. According to the information provided by the government of Región de Murcia under its energy saving initiative "Ecorresponsabilidad" [26], a laptop consume around 0,11kW, which means approximately 99kWh along the 24 weeks of the project.
Also based on the information provided by the murcian government, each kWh consumed in Spain emit approximately 0,343 Kg of CO_2 to the atmosphere. In other words, the environmental footprint associated to the use of the laptop for developing this project has been approximately 33,957 Kg of CO_2.

Appendix D

Social Impact

To summarize the social impact expected of coordinated vehicles, the area of attention has been set over the improvements in quality of life expected from autonomous vehicles, which is the main technology which will take advantage of coordination techniques.

D.1 Social Impact of Autonomous Vehicles

From the point of view of the social impact, many aspects should be commented. First of all and related with previous Chapter C, an improvement of the air quality and the noise pollution is directly translated into an improvement of the health of the citizens. Nevertheless, a transition into autonomous vehicles will have many other positives aspects noteworthy.

On one hand, a more efficient mobility will reduce time spent at vehicles, and reducing traffic jams and avoid the driving, is expected to reduce the stress levels of the population.
Besides, autonomous cars would not only improve the quality of life of the citizens, but also would democratize the transport by reaching people who would not get access to a car if they were not autonomous such as underage people or those who cannot get a drive license due to medical adversities increasing the safety of people turning back home or their range of socials and employment possibilities being able to get to new places without depending on others.
Inside the multiple possibilities of autonomous vehicles are also public or at least shared vehicle fleets reducing the number of cars on the streets reducing the difficulty of finding a parking place, and decreasing the personal investment in vehicles maintenance being affordable for people with not many resources.
Finally, the most important aspect to be mentioned is the main objective of this project, which is save human lives by reducing traffic accidents.

Bibliography

[1] Robin Verschueren et al. "Towards time-optimal race car driving using nonlinear MPC in real-time". In: *53rd IEEE conference on decision and control* (Dec. 2014), pp. 2505–2510.

[2] Teodoro Alamo, José Manuel Bravo, and Eduardo F Camacho. "Guaranteed state estimation by zonotopes". In: *Automatica* 41.6 (2005), pp. 1035–1043.

[3] Eugenio Alcalá, Vicenç Puig, and Joseba Quevedo. "LPV-MP planning for autonomous racing vehicles considering obstacles". In: *Robotics and Autonomous Systems* 124 (2020), p. 103392.

[4] Eugenio Alcalá et al. "Fast zonotope-tube-based LPV-MPC for autonomous vehicles". In: *IET Control Theory & Applications* 14.20 (2020), pp. 3676–3685.

[5] Eugenio Alcalá Baselga. "Advances in planning and control for autonomous vehicles". In: (2020).

[6] Matthew Barth and Kanok Boriboonsomsin. "Real-world carbon dioxide impacts of traffic congestion". In: *Transportation research record* 2058.1 (2008), pp. 163–171.

[7] André M Carvalho and Joao S Sequeira. "Approximating Viability Kernels of Non-linear Systems." In: *ICINCO (2)*. 2018, pp. 343–350.

[8] Claus Danielson et al. "Robust motion planning for uncertain systems with disturbances using the invariant-set motion planner". In: *IEEE Transactions on Automatic Control* 65.10 (2020), pp. 4456–4463.

[9] Ali Gohar and Gianfranco Nencioni. "The role of 5G technologies in a smart city: The case for intelligent transportation system". In: *Sustainability* 13.9 (2021), p. 5188.

[10] M. Herceg et al. "Multi-Parametric Toolbox 3.0". In: *Proc. of the European Control Conference*. `http://control.ee.ethz.ch/~mpt`. Zürich, Switzerland, 2013, pp. 502–510.

[11] Robert Hult et al. "Coordination of cooperative autonomous vehicles: Toward safer and more efficient road transportation". In: *IEEE Signal Processing Magazine* 33.6 (2016), pp. 74–84.

[12] Jason Kong et al. "Kinematic and dynamic vehicle models for autonomous driving control design". In: *2015 IEEE intelligent vehicles symposium (IV)*. IEEE. 2015, pp. 1094–1099.

[13] Pantelis Kopelias et al. "Connected & autonomous vehicles–Environmental impacts–A review". In: *Science of the total environment* 712 (2020), p. 135237.

[14] "Ley 27/2014, de 27 de noviembre, del Impuesto sobre Sociedades." In: *BOE* 288 (2014), pp. 96939–97097.

[15] Alexander Liniger and John Lygeros. "Real-time control for autonomous racing based on viability theory". In: *IEEE Transactions on Control Systems Technology* 27.2 (2017), pp. 464–478.

[16] J. Löfberg. "YALMIP : A Toolbox for Modeling and Optimization in MATLAB". In: *In Proceedings of the CACSD Conference*. Taipei, Taiwan, 2004.

[17] Stefanie Manzinger, Christian Pek, and Matthias Althoff. "Using reachable sets for trajectory planning of automated vehicles". In: *IEEE Transactions on Intelligent Vehicles* 6.2 (2020), pp. 232–248.

[18] MATLAB. *version 9.12.0.1884302 (R2022a)*. Natick, Massachusetts: The MathWorks Inc., 2022.

[19] Niklas Kochdumper Matthias Althoff and Mark Wetzlinger. " CORA 2021 Manual". In: `https://tumcps.github.io/CORA/`. Technische Universität München, 85748 Garching, Germany, 2021.

[20] András Mihály et al. "Performance Analysis of Model Predictive Intersection Control for Autonomous Vehicles". In: *IFAC-PapersOnLine* 54.2 (2021), pp. 240–245.

[21] Ian M Mitchell, Jacob Budzis, and Andriy Bolyachevets. "Invariant, viability and discriminating kernel under-approximation via zonotope scaling". In: *Proceedings of the 22nd ACM International Conference on Hybrid Systems: Computation and Control*. 2019, pp. 268–269.

[22] C Ocampo-Martinez et al. "Actuator fault-tolerance evaluation of linear constrained model predictive control using zonotope-based set computations". In: *Proceedings of the Institution of Mechanical Engineers, Part I: Journal of Systems and Control Engineering* 221.6 (2007), pp. 915–926.

[23] Philip Polack et al. "The kinematic bicycle model: A consistent model for planning feasible trajectories for autonomous vehicles?" In: *2017 IEEE intelligent vehicles symposium (IV)*. IEEE. 2017, pp. 812–818.

[24] Rajesh Rajamani. *Vehicle dynamics and control*. Springer Science & Business Media, 2011.

[25] "Real Decreto 1125/2003, de 5 de septiembre, por el que se establece el sistema europeo de créditos y el sistema de calificaciones en las titulaciones universitarias de carácter oficial y validez en todo el territorio nacional." In: *BOE* 224 (2003), pp. 34355–34356.

[26] Consejeria de agricultura y agua Region de Murcia. *Uso del ordenador portatil vs ordenador de sobremesa*. URL: `http://www.ecorresponsabilidad.es/fichas/portatil.htm`.

[27] "Resolución de 28 de febrero de 2019, de la Secretaría de Estado de Función Pública, por la que se dictan instrucciones sobre jornada y horarios de trabajo del personal al servicio de la Administración General del Estado y sus organismos públicos." In: *BOE* 52 (2019), pp. 19756–19766.

[28] David Rojas-Rueda et al. "Autonomous vehicles and public health". In: *Annual review of public health* 41.1 (2020), pp. 329–345.

[29] Jeff S Shamma. "An overview of LPV systems". In: *Control of linear parameter varying systems with applications* (2012), pp. 3–26.

[30] Yuanyuan Wu, Haipeng Chen, and Feng Zhu. "DCL-AIM: Decentralized coordination learning of autonomous intersection management for connected and automated vehicles". In: *Transportation Research Part C: Emerging Technologies* 103 (2019), pp. 246–260.

[31] Ibrar Yaqoob et al. "Autonomous driving cars in smart cities: Recent advances, requirements, and challenges". In: *IEEE Network* 34.1 (2019), pp. 174–181.

[32] Betina Carol Zanchin et al. "On the instrumentation and classification of autonomous cars". In: *2017 IEEE International Conference on Systems, Man, and Cybernetics (SMC)*. IEEE. 2017, pp. 2631–2636.

[33] Majid Ghaniee Zarch et al. "Process performance verification using viability theory". In: *Processes* 9.3 (2021), p. 482.